ERA 71-3

HYBRID WATER IMMERSION SIMULATION OF MANUAL IVA PERFORMANCE IN WEIGHTLESSNESS

By Harry L. Loats, Jr. and G. Samuel Mattingly

NAS9-12122

DRL Number: T-719

Line Item Number: 4

Environmental Research Associates
Essex, Maryland

15 December 1971

ERA 71-3

HYBRID WATER IMMERSION SIMULATION OF MANUAL IVA PERFORMANCE IN WEIGHTLESSNESS

By Harry L. Loats, Jr. and G. Samuel Mattingly

NAS9-12122

DRL Number: T-719

Line Item Number: 4

Environmental Research Associates
Essex, Maryland

15 December 1971

TABLE OF CONTENTS

TABLES

FIGURES

HYBRID WATER IMMERSION SIMULATION OF MANUAL IVA PERFORMANCE IN WEIGHTLESSNESS

By Harry L. Loats, Jr. and G. Samuel Mattingly
Environmental Research Associates

1.0 INTRODUCTION

The technical effort in this contract was divided, approximately equally, into two areas. The first area, Simulator Development, involved the final portion of the development of a simulator concept which was begun under a previous contract (NAS1-8975-2), e.g., a hybrid water immersion motion simulator for investigating manual human performance in simulated weightlessness. The second area, Operational Task Demonstration, involved utilizing the simulator to evaluate specific tasks to be performed in weightlessness and to provide data concerning manual human performance.

The simulator, generally known as the Cargo Transport Simulator or CTS, was originated by Environmental Research Associates, and comprises a hybrid simulator using a combination of water immersion and mechanical, Peter Pan, simulation to attain the benefits of the tractionlessness of water immersion without paying the penalties of drag and planing forces. The concept operates on the equivalence principle--instead of the test subject and cargo moving along some form of motion aid, the subject and cargo remain quasi-stationary and the motion aid is moved. The motion aid is controlled by a servo system which responds to the forces applied by the test subject. Computation of the inertial movement in a weightless state results in correct motion response. Since the subject and cargo remain essentially fixed, viscous and hydrodynamic forces are reduced significantly, yet the simulator retains the primary advantage of water immersion (simulated weightlessness and a full six-degrees-of-freedom). The concept, in general, allows measurements of the forces applied by a test subject on motion aids as he

translates from one location to another. A test series was planned and conducted in which a test subject accelerated himself and additional simulated masses along a continuous rope motion aid.

The second area, Operational Task Demonstration, involved a review of future mission tasks, particularly those tasks associated with Skylab, and the application of the simulator concept to selected tasks. This area resulted in the analysis and experimental evaluation of estimated Skylab station-to-station timelines and the selection and simulation of the FCMU-T013 manual motion arrest task. Simulator test data was evaluated against currently established mission timelines, and the mission task demonstration selected for simulation was manual arresting of the Foot Controlled Maneuvering Unit Experiment (T020) by the safety man. The safety man's position, as defined in the experiment, was changed to agree with a recommended experiment modification in which the safety man is located in the foot restraints of the force platform of Experiment T013.

A specific area of interest during the program was to be the identification of "threshold" forces during task performance. As the contract progressed, it became apparent that there exists a family of thresholds. These were defined during the program in terms which will allow specific measurements to be made using a version of the CTS.

This document contains a description of the simulator development, test data and analysis, and general conclusions concerning manual mass handling and translation in weightlessness.

2.0 SIMULATION

Future space operations will require manual transfers of a large variety of cargo under both intravehicular and extravehicular conditions. In order to determine the techniques, human factor considerations, assistive devices, package limitations, training procedures, etc., related to the cargo transfer problem, extensive ground-based simulation is required.

Two simulation techniques, water immersion and zero-G aircraft, have proven effectivity for selected simulated weightless tasks, particularly static tasks. The utilization of water immersion was shown to be of definite value in the Gemini EVA task performance. The use of the zero-G aircraft for astronaut training and acclimatization is well documented. When mass cargo transfer in weightlessness is simulated, however, results of simulations in the two modes show a significant difference. The reasons for disagreement are to be found in the limitations of the techniques and how the specific results are interpreted.

In the zero-G aircraft studies of cargo transfer, the major problems influencing simulation results are the limited test time and the small, but important, variations in "G" forces during the parabolic trajectory. The latter effect produces an unstable reference frame and spurious accelerations. Results of studies using motion aids on mock-ups attached to the aircraft are seriously degraded. Because of these problems, realistic quantative data has been difficult to obtain.

The major problem encountered in water immersion studies of cargo transfer is caused by viscous drag on the men and cargo. This effect influences the orientation of both subject and cargo during maneuvers and unrealistically damps out motions. These anomalies seriously affect the validity of the data obtained. In the past, considerable effort has been expended to alleviate the problems

associated with viscous drag. This effort has included hydrodynamic shaping of masses, limiting the speed at which tasks were done, and analysis of drag effects to determine experiment degradation. These artifices notwithstanding, drag is still a major concern and performance constraint, particularly as regards quantitative measures of performance.

The Cargo Transport Simulator (CTS) concept was originated by Environmental Research Associates (ERA)--partially developed under contract to NASA Langley Research Center (LRC) and completed on this contract. The concept operates on the equivalence principle. Instead of the test subject and cargo moving along some form of motion-transfer aid, the subject and cargo remain stationary and the transfer aid is moved. The motion-transfer aid used is a continuous 3/8 in. diameter rope. However, other types of aids, such as handrails, surfaces, etc., can be provided for future test programs. Since the subject and cargo remain essentially fixed, viscous forces are virtually nonexistent, yet the simulator retains the primary advantages of the capability of extended time water immersion of full six-degrees-of-freedom movement. Figure 1, General Arrangement--Cargo Transport Simulator, is a schematic representation of the CTS mechanical equipment arrangement. Using this technique, actual cargo sizes, masses, etc., can be investigated, and quantitative data on subject force inputs, subject/-cargo c.g. motion, transfer velocities, etc., can be obtained.

The following events occur in a typical operational cycle using the Cargo Transport Simulator. The subject starts the cargo transfer maneuver by applying a force to the motion aid (Figure 2-A). This force is the same as would occur if the transfer aid were fixed and the subject free to move. This force, and other later force inputs, are sensed by load cells (Figure 2-B) and produce signals which are processed by the analog computer (Figure 2-C) to produce a signal proportional to the relative velocity of the

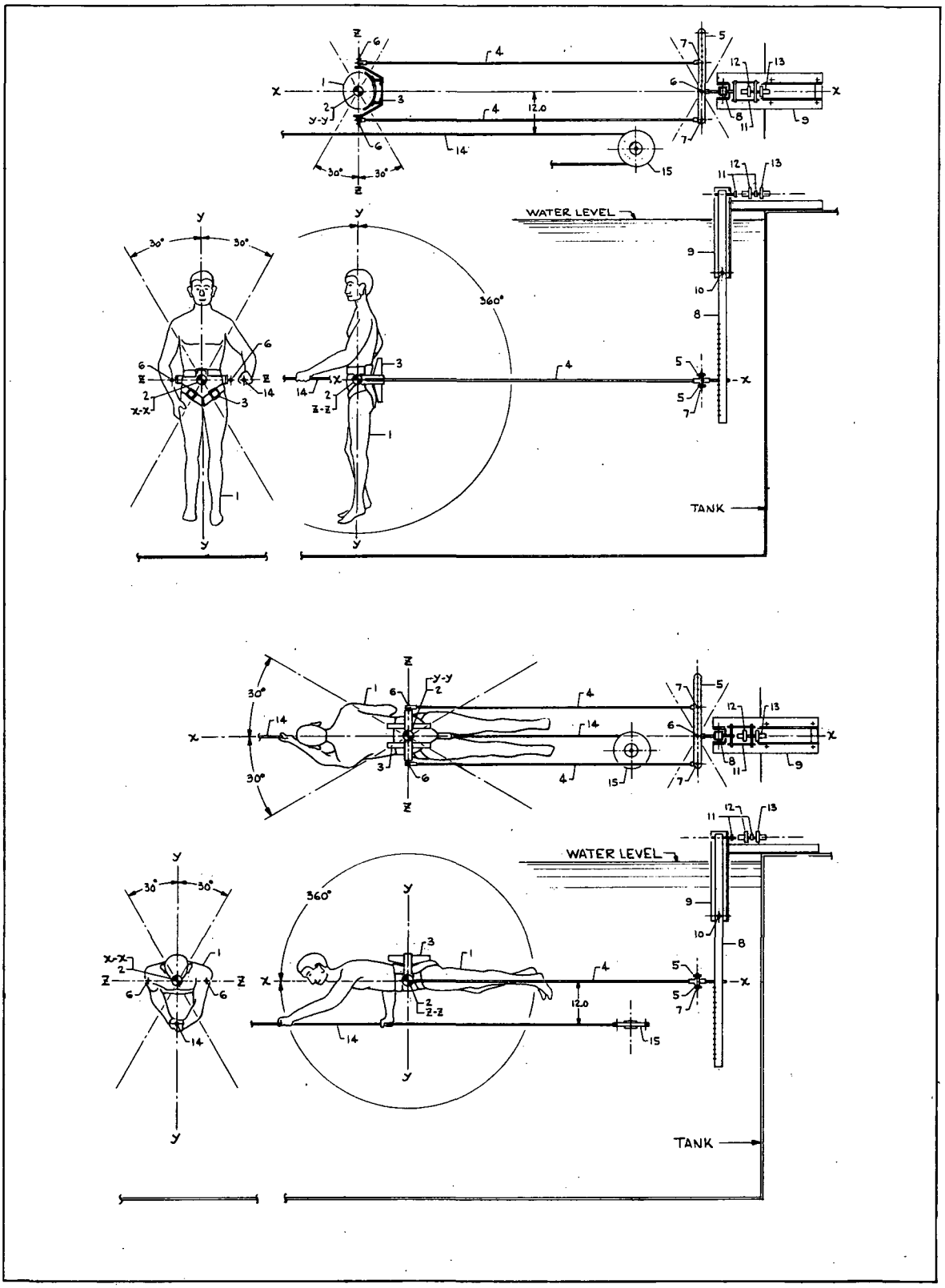

FIGURE 1 - GENERAL ARRANGEMENT--CARGO TRANSPORT SIMULATOR

LEGEND
1 SUBJECT 2 MASS CENTER - SUBJECT 3 SADDLE - SUBJECT 4 TIE ROD 5 TIE BAR 6 BALL JOINT 7 PIN JOINT 8 FULCRUM BAR 9 SUPPORT - FULCRUM BAR AND LOAD CELLS 10 PIVOT - FULCRUM BAR 11 LOAD LINK 12 LOAD CELL AND TRANSDUCER (PUSH) 13 LOAD CELL AND TRANSDUCER (PULL) 14 TOW LINE 15 IDLER PULLEY - TOW LINE
NOTES
1. ANGLES INDICATE UNRESTRICTED DEGREES OF FREEDOM IN ROLL, PITCH, AND YAW FOR SUBJECT ABOUT HIS MASS CENTER. 2. SUBJECT IS FREE TO MOVE, ABOUT BALL JOINT (6) BETWEEN TIE BARS (5), VERTICALLY AND HORIZONTALLY ALONG THE Y AND Z AXES RESPECTIVELY, BUT IS RESTRAINED, THRU THE LOAD CELLS (12 AND 13), FROM MOVING HORIZONTALLY ALONG THE X AXIS. ANGULAR MISALIGNMENT OF THE X AXIS THRU BALL JOINT (6) IS KEPT AT A MINIMUM BY SHIFTING SUPPORT (9) VERTICALLY AND HORIZONTALLY ONCE SUBJECT MASS CENTER (2) HAS BEEN DETERMINED IN RELATION TO TOW LINE (14).

FIGURE 1 - GENERAL ARRANGEMENT--CARGO TRANSPORT SIMULATOR--CONTINUED

subject/cargo and the fixed system (i.e., spacecraft). This signal drives the servo motor (Figure 2-D) which in turn powers the maneuvering aid.

As the subject's force inputs continue, the velocity of the motion aid increases proportional to the integral of the impressed forces. When no force is produced by the subject, the resulting constant velocity is maintained by the servo motor. This relative motion between aid and subject is identical to that occurring in space, and will continue until deceleration is effected. When deceleration is effected, the subject grasps the aid and starts braking either rapidly or gradually--the velocity of the motion aid decreases as this braking occurs. Figure 3 is a functional block diagram of the analog computer circuit described above. Figure 4 shows the CTS motor control circuit.

The control signals produced, as well as the corresponding accelerations and velocities, are continuously recorded. For the test series used for data in this contract a 4 channel REAC recorder was used. Figure 5 shows 3 test runs performed consecutively within a period of 10 min. The test subject was instructed to compare the mass of each run with the previous run on a basis of greater-lesser-equal to. The simulated mass was then held constant at a total of 7 slugs. The subjective comparison was "slightly greater or approximately equal" for each run. The next run, immediately following, had a simulated mass of 35 slugs, and is shown in Figure 6. The subjective comment was that there was "infinitely greater mass." It can be seen that the subject was able to perform repeatable runs even though he was purposely kept unaware of the exact mass sequence to be followed. The small variation to the average acceleration and peak velocities showed that the subject could easily use the velocity of the mass as information feedback to properly control the maneuver. The data from the strip chart recording was reduced and plotted to ascertain

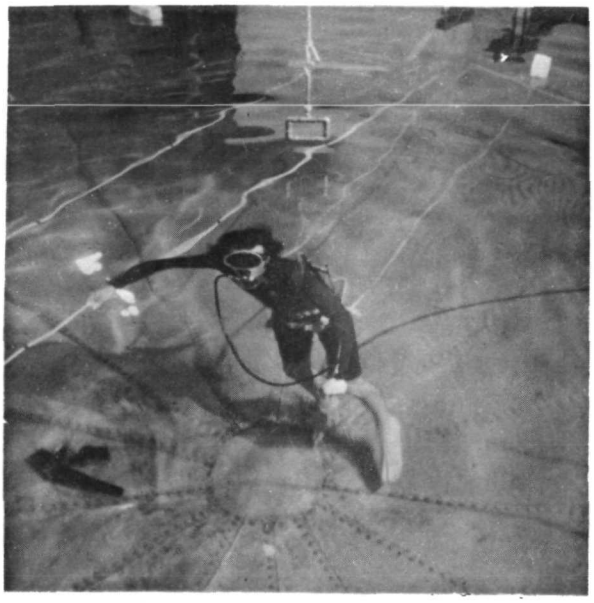

(A) SUBJECT POSITION

(C) COMPUTER RECORDER STATION

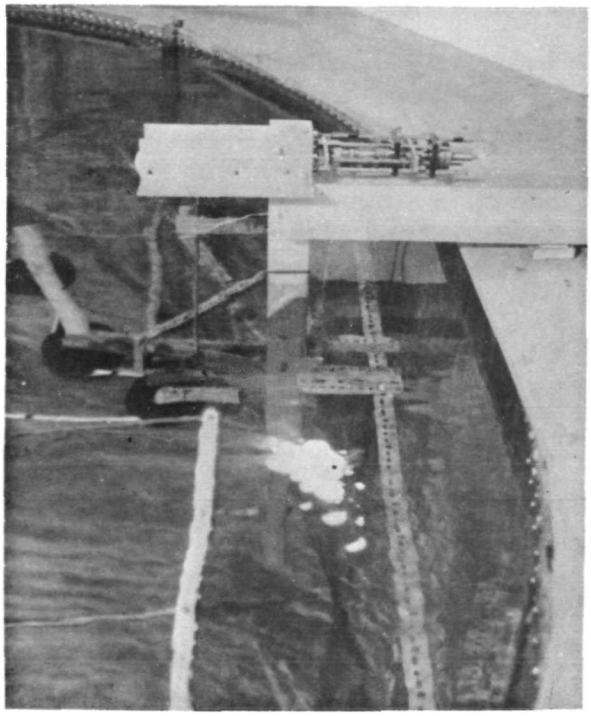

(B) FORCE SENSING LOAD CELLS

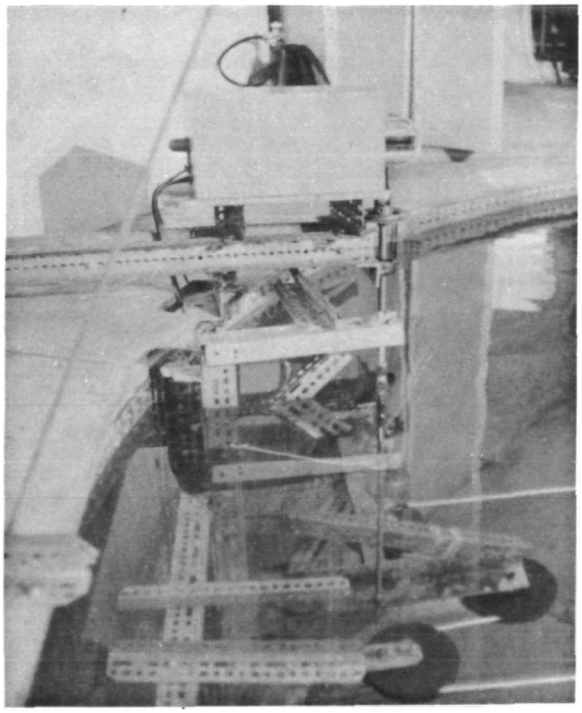

(D) SERVO DRIVE SYSTEM

FIGURE 2 - MAJOR CTS COMPONENTS/ARRANGEMENTS

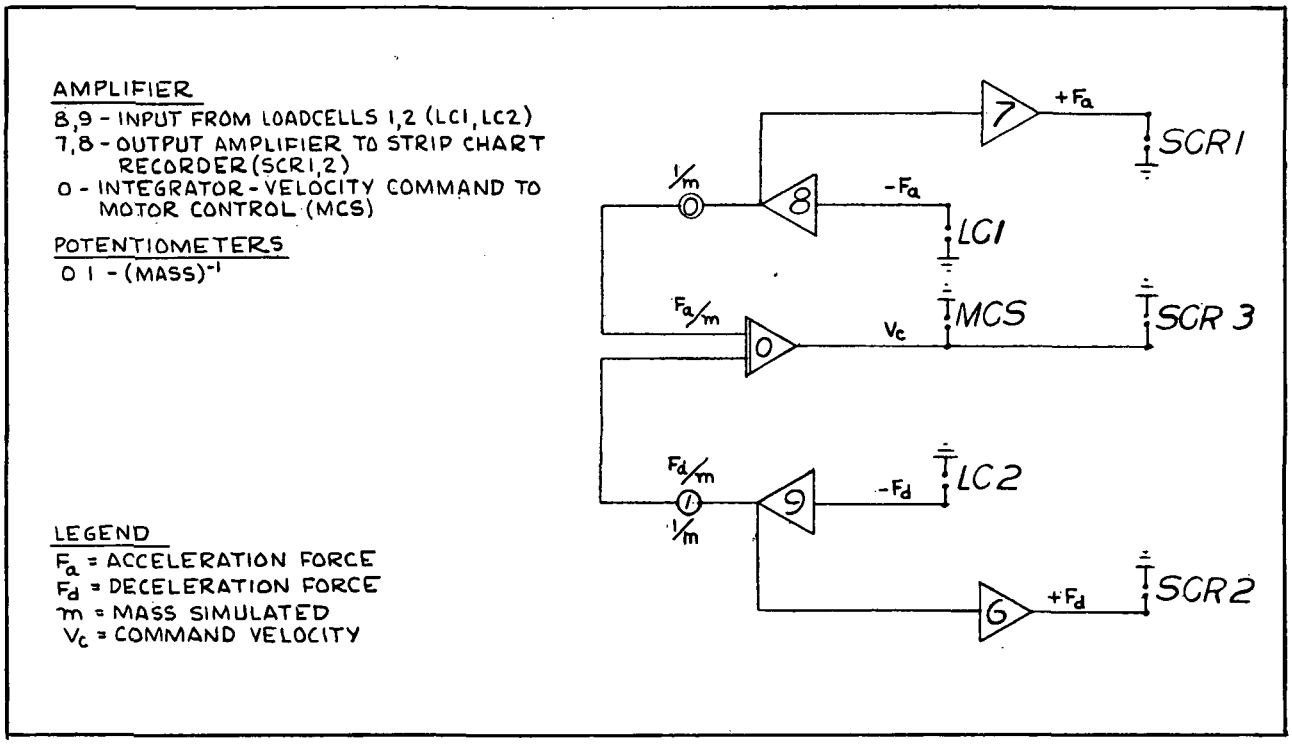

FIGURE 3 - CTS ANALOG COMPUTER CIRCUIT

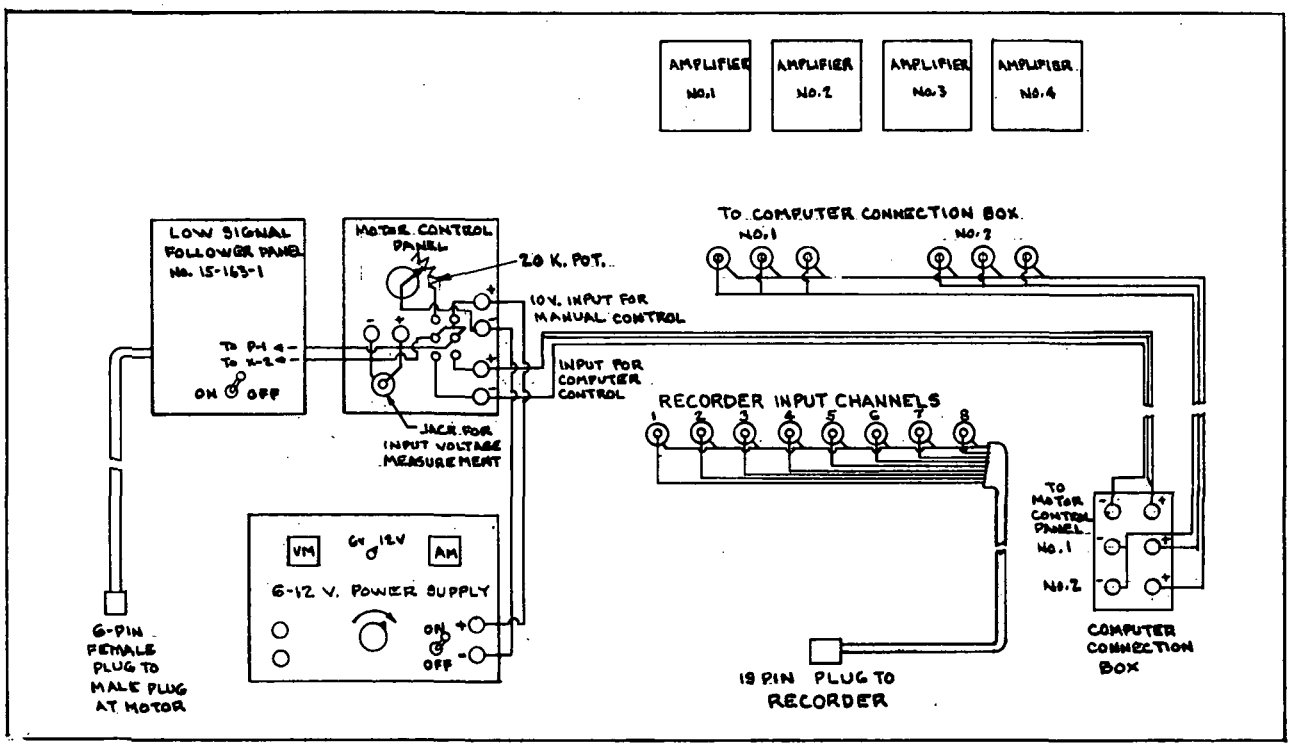

FIGURE 4 - CTS WIRING DIAGRAM--MOTOR CONTROL

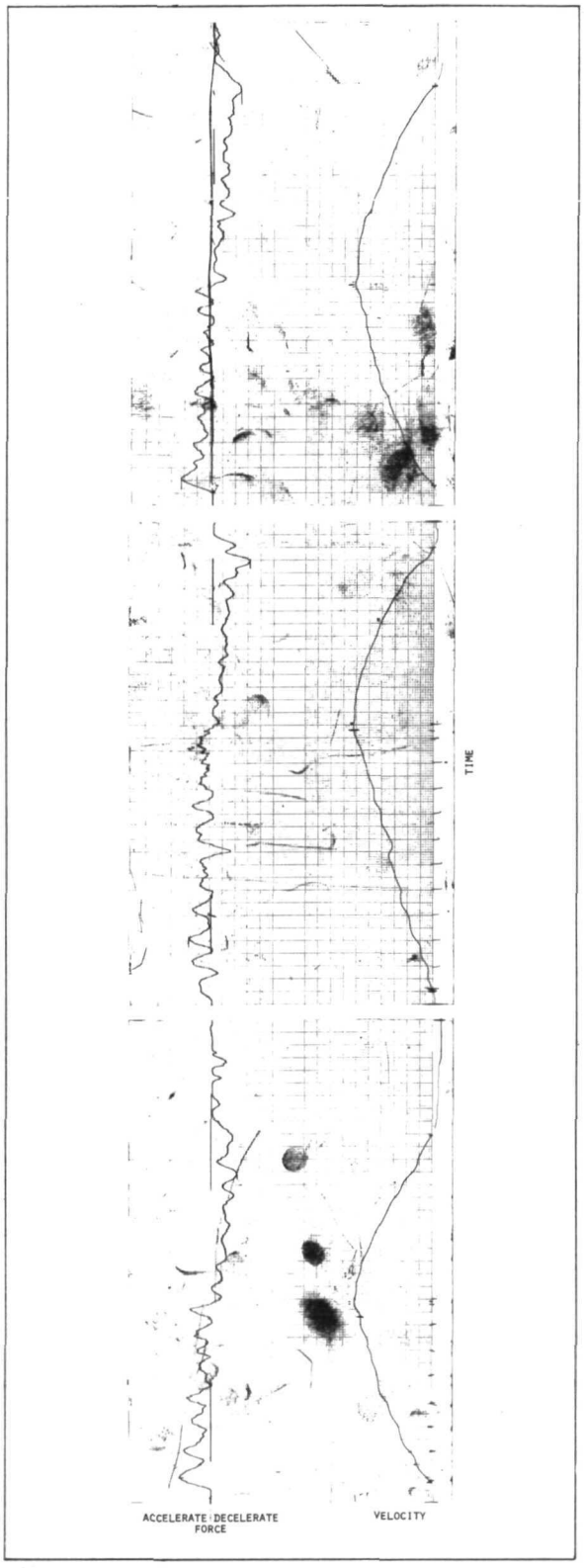

FIGURE 5 - REPETITIVE LOW MASS TEST RUNS

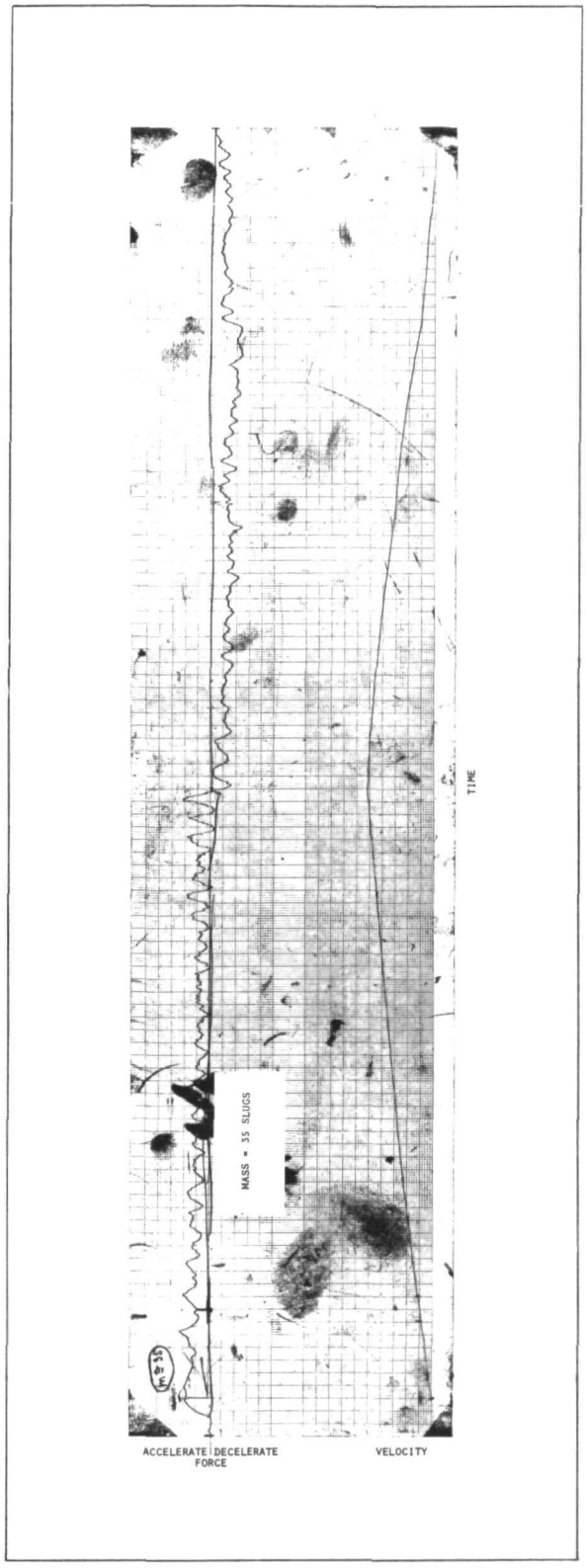

FIGURE 6 - HIGH MASS TEST RUN

significant characteristics or trends associated with the systematic variation of the test parameters.

During all of the maneuvers, the relative motion of the subject and cargo, i.e., out-of-plane motion, pitch, yaw, and roll, occurs essentially uninhibited (because of the low rates). In addition to providing a realistic simulation of cargo transfer, the mechanization and use of the computer allow recording and analysis of force inputs, resultant velocities and distances, subject and cargo motions, etc. In general, the force profiles and resultant accelerations and velocities do not differ significantly from the anticipated profiles projected analytically prior to beginning the actual test.

3.0 CARGO TRANSFER EXPERIMENTS

3.1 Cargo Transfer Experiment Discussion and Observations

In order to move from one position to another in weightlessness without the use of thrusters, an astronaut must apply a manual force against a motion aid to effect the desired acceleration of his mass plus any additional mass of cargo being transported. Additionally, he must apply controlled body-torque if the force applied is not directly in line with the center of mass of the system (man and cargo).

The physiological mechanisms by which a human subject applies forces for acceleration and body-torques are not the concern of this contract. This contract is concerned with the magnitude of the forces applied, the time-profiles of force application, the frequency of force applications, and the resultant motions of both the subject and his cargo. Since the acceleration of known masses resulting from the application of known forces can be calculated, the problem can be resolved into measuring the application of force by the subject in the dynamic condition and causing the resultant analytically determined motion of the combined subject and cargo mass. We have measured these force applications and developed a basic body of information concerning human performance during manually induced motion in weightlessness. This information relates also to the requirement for structural integrity and frequency of placement of motion aids. It further provides experimental data in support of timeline prediction and on human capabilities to provide motive forces for transportation of cargo.

From the results of previous contracts, in particular contract NAS1-7887 under which the Cargo Transport Simulator concept was first demonstrated, it was anticipated that the magnitude of the forces applied by human subjects would be relatively low, i.e., less than 100 lb. This is obvious when one considers that the

average astronaut-subject is less than a 6-slug mass, and that a 6 lb force would accelerate that mass at a rate of 1 ft/sec^2. The simulator was designed to measure forces in the ± 100 lb range. The masses under consideration were a minimum of 5 slugs (160 lb astronaut) to 15 slugs (160 lb astronaut with 320 lb additional cargo). This range covers all the practical requirements of cargo transfer presently planned for the Skylab missions. The practical dynamic range of the CTS was 1-300 in mass, and a limited number of test runs were made with the subject accelerating and decelerating masses of 100 slugs (3200 lb wt).

A harness was designed and built which allowed the subject to assume a position normal to the rope motion aid and apply accelerating and decelerating forces with one hand. It had been anticipated that this would be accomplished within a maximum yaw of ± 30°. It was found, however, that the subject exceeded 30° yaw, and constantly interacted the stops of the harness structure. The harness was then modified so that the subject was aligned with the rope motion aid and used both hands in acceleration and deceleration. This resulted in complete freedom of operation.

Two techniques were used to measure the forces. In the first, the harness support was attached to the structure of the pool through a load cell arrangement capable of sensing forces in the ± 100 lb range. In this technique, as the subject applies an acceleration force to the rope motion aid, the load cells sense this force and supply a signal to the analog computer which processes the signal and activates the servo mechanism. The other general technique used for measuring the forces is to position the load cells to sense tension at either end of the rope motion aid. An accelerating force on the line increases the tension sensed by the load cell in front of the subject and decreases the tension sensed by the load cell behind the subject. These signals are compared by the analog computer. The resultant signal is as an increase in voltage in a similar fashion to the previous method. System

calibration consists of applying a known fixed load to the load cells and measuring the constant slope of the velocity output curve. Different slopes, e.g., different simulated masses, are obtained by setting an appropriate potentiometer which feeds the main integrator.

Test runs were made using both techniques. Each technique, however, has limitations and degradations. In the first technique, sensing from the subject harness, the load cell sensors see all the forces put in by the subject, including forces resulting from the motion of his arms through the water. The second technique, load cell sensors at either end of the rope motion aid, is more realistic in that it "sees" only the component of force actually applied to the motion aid. It has difficulty, however, in that it is very sensitive to noise level caused by any discontinuity in the rope itself, such as a splice. Although there are computer techniques and equipment available to reduce this background noise level, it was decided to use the first measurement technique, in that comparative tests using each technique showed approximately the same profiles and force levels. A technique to eliminate this noise was developed for subsequent operations and involves analog filtering techniques.

Although the data test runs included a variety of simulated mass levels, e.g., the system response was adjusted to the total mass of the subject and cargo, no additional real cargo package mass was added to the subject. Some additional fidelity could possibly be gained in future tests by the addition of neutrally buoyant cargo attached to the test subject so that his motion around his mass center not controlled by the simulator would be more precise. The point of attachment of the subject to the simulator was altered to simulate the displacement of the system center of mass to a maximum of 6 in. outboard of the subject's actual mass center. Tests were performed in which the subject was accelerating and

decelerating a total 10-slug mass, and the position of attachment of the harness was such that the subject would pitch, roll, and yaw about a point 6 in. outboard of his natural mass center as if he had an additional mass attached to his back, thus yielding the system mass center at that point.

Instructions to the subject were brief, and appear in Table I, Neutral Buoyancy Test Plan: Cargo Transport. There appears to

TABLE I.--NEUTRAL BUOYANCY TEST PLAN: CARGO TRANSPORT

MODE: IVA
TRAVEL PATH: LINEAR
MOTION AID: CABLE
INDEPENDENT VARIABLE: $F_X(t)$--APPLIED FORCE MEASURED THRU C.G.
DEPENDENT VARIABLE: $\ddot{X}(t)$--ACCELERATION OF THE CARGO/-SUBJECT C.M.
PARAMETERS: M_C--CARGO MASS (0, 2, 4, 6, 8, 10 SLUGS) C.G.--CENTER OF MASS LOCATION (0, 3, 6 IN.) MODE--BODY ALIGNED WITH ROPE (TWO HANDS) BODY ALIGNED NORMAL TO ROPE (ONE HAND)
DATA ANALYSIS AND TREATMENT: A LATIN SQUARE TEST DESIGN PRINCIPLE WILL BE USED AS A MEANS OF FIRST ORDER BALANCING THE EFFECT OF INDIVIDUAL DIFFERENCES AND ORDER OF TESTING.
INSTRUCTIONS TO THE SUBJECT: THE SUBJECT IS INSTRUCTED TO ACCELERATE AND DECELERATE WHILE MAINTAINING BODY POSITION; THAT IS, TO AVOID TWISTING THE BODY IN EITHER YAW OR PITCH. IT IS UNDERSTOOD THAT THIS REDUCES THE SUBJECT'S ABILITY TO APPLY MAXIMUM FORCE ON THE MOTION AID. AS THE MASS CENTER OF THE SYSTEM MOVES OUT FROM THE SUBJECT'S MASS CENTER, IT IS ANTICIPATED THAT THE SUBJECT WILL FIND IT MORE DIFFICULT TO APPLY FORCE TO THE MOTION AID, AND THAT THERE WILL BE SOME YAWING MOTION, AND THAT THE TENDENCY TO YAW WILL INCREASE WITH THE INCREASING SHIFT OF THE MASS CENTER. A SUBJECTIVE EVALUATION OF THIS PROBLEM WILL BE INCLUDED IN THE TEST RESULT REPORTS.

be a short learning period during which the subject's initial motions visually appear erratic and discontinuous. The resultant data mirrors this effect. No attempt was made during this contract to establish a learning curve. After a few days of test runs, the subject performance appeared to stabilize. It should be noted that a review of the Apollo onboard films in some cases shows a similar change from jerky motions and a low level of confidence early in a flight to a much smoother and confident performance later in the same flight.

Three test subjects were used for system checkout. All three have several years experience in water immersion simulation, including pressure suit simulation work during the Gemini program. Two subjects, in addition, have had experience both suited and unsuited in the zero-gravity aircraft. The most significant subjective comments are as follows:

> "There is an eerie feeling of motion induced by the simulator if one closes his eyes during the acceleration. Your mind knows that you're not moving and yet you feel like you're going to bounce into the tank at any second. The feeling is similar to soaring in the zero-gravity aircraft, and not at all like moving through the water."
>
> "It is difficult, if not impossible, to determine how much mass one is accelerating. It is simple to determine that a test run of a 50-slug mass following a test run of a 5-slug mass is a much higher mass, but their actual relative values would be strictly a guess."
>
> "There is much more to deceleration than there is to acceleration. It becomes more difficult to apply a controlled deceleration at higher velocities. It is also more difficult to provide a controlled deceleration in tests where the point of attachment is shifted behind the test subject."

"I don't know how hard I was pulling, probably 20 or 30 lb."

"As you pull on the line, you have a definite tendency to get closer to the line as if your mass center wants to line up with it."

"Trying to decelerate from a comparative high velocity while using only one hand appears to be almost impossible."

It was further observed that a test subject with some experience on the simulator acting as an external observer could make reasonably accurate guesses as to the mass levels simply by watching the acceleration of the subject motions, but could not attain the same accuracy while acting as a subject. Apparently, the subject is engrossed in the problems of body control, and thus cannot accurately determine the simulated mass, while an observer can concentrate solely on acceleration and, since the rate of acceleration is directly proportional to mass level, he can make a reasonably accurate guess as to the mass level simulated.

The observers also noticed that in all cases the subject had a tendency to bring his mass center closer to the line during acceleration. The subject actually pitched up so that his legs straddled the rope motion aid during acceleration; the opposite occurred during deceleration. These tendencies appeared more pronounced with the increase in simulated mass and also with the location of the restraint point moved outboard the subject's center of mass.

Figure 7-A depicts the subject in line with the motion aid, with his point of attachment (mass center) at a position 12 in. from the motion aid and one hand grasping the rope. At the instant of application of an accelerating impulse, the motion aid is subject to an in-line force (R_1). For the purpose of discussion, let us give this force a value of 10 lb (the approximate mean value of accelerating forces during a typical test run, 1015-3). The test subject experiences an equivalent 10 lb force (F_1) at his center

of mass. The magnitude of the resultant force vector taken from the point of attachment through the mass center (F_4) is 10.54 lb. In order to maintain a position of 12 in. above the motion aid, the subject would have to apply a counter-torque (M) at the point of attachment of 120 in-lb. Our experiments indicate that the test subjects do not apply equilibrium torque, and as a result the mass center, or center of gravity of the subject, tends to move toward the motion aid.

If there were no counter-torque applied at the point of attachment, the instantaneous force (F_3) moving the center of mass of the subject toward the motion aid would be approximately 3.3 lb. Under these conditions, the subject with no additional mass would reach a point shown in Figure 7-B, approximately 1.5 sec. For another in-line force of 10 lb (a second stroke), the tendency of the mass center to move toward the motion aid continues, but at a reduced magnitude. Analysis of the force vectors supports what was deduced from observation of the tests--the mass center of the subject has a tendency to align with the motion aid during acceleration. This is a stabilizing force, as the subject is actually closer to the motion aid and more able to maintain control. Additional analysis, however, shows that it is equally true, but not quite so obvious, that a decelerating force has a tendency to move the subject's mass center away from the motion aid, and tends to create an unstable situation where the subject has less control, thereby reducing performance. Heretofore, most analysis has led to the conclusions that acceleration and deceleration were symmetric in nature since the total energy provided for acceleration must be the same total energy provided for deceleration; i.e., man can decelerate any mass that he can accelerate. This analysis supports the subjective comment of greater difficulty in decelerating than accelerating.

Figure 7-B illustrates the position of the subject after one or more strokes have been completed, and he has allowed his mass center

to approach the motion aid as closely as possible (4 in.). This illustration is at the instant of force application for an additional stroke. The major differences in the forces as noted are the reduction in the torque required at the wrist to maintain equilibrium, or if no torque is applied, a reduction in the force tending to accelerate the subject's mass center toward the motion aid.

Figure 7-C is a comparable illustration to Figure 7-A except that the subject's center of mass, or center of gravity, has been altered to a point 6 in. outboard as if the system mass center were at that point. (This is accomplished in the simulator by moving the point of attachment 6 in. and allowing the subject to roll, pitch, and yaw around that point.) Using the same in-line force of 10 lb, the actual mass center of the subject 12 in. from the rope as in Figure 7-A but with the new system center of mass 18 in. from the rope, it can be seen that the torque requirement at the subject's wrist, or the force tending to move the subject toward the motion aid, has been significantly increased. Since decelerating forces would be the same as accelerating forces, except in the reverse direction, a comparison of the situations depicted in Figures 7-A and 7-C supports the subjective comment that it is increasingly difficult to provide a controlled deceleration as the system's mass center (point of attachment) is shifted outboard.

Figure 7-D depicts the situation when the subject has both hands in contact with the motion aid, and is thus able to maintain a position of 12 in. relative to the motion aid by using one arm in tension and one arm in compression. At this point the subject is actually using both hands to form a "box-beam" and distributes the loads so as to provide counter-torque by the position of the two hands. During acceleration this is actually not very significant since the motion being resisted merely tends to move the

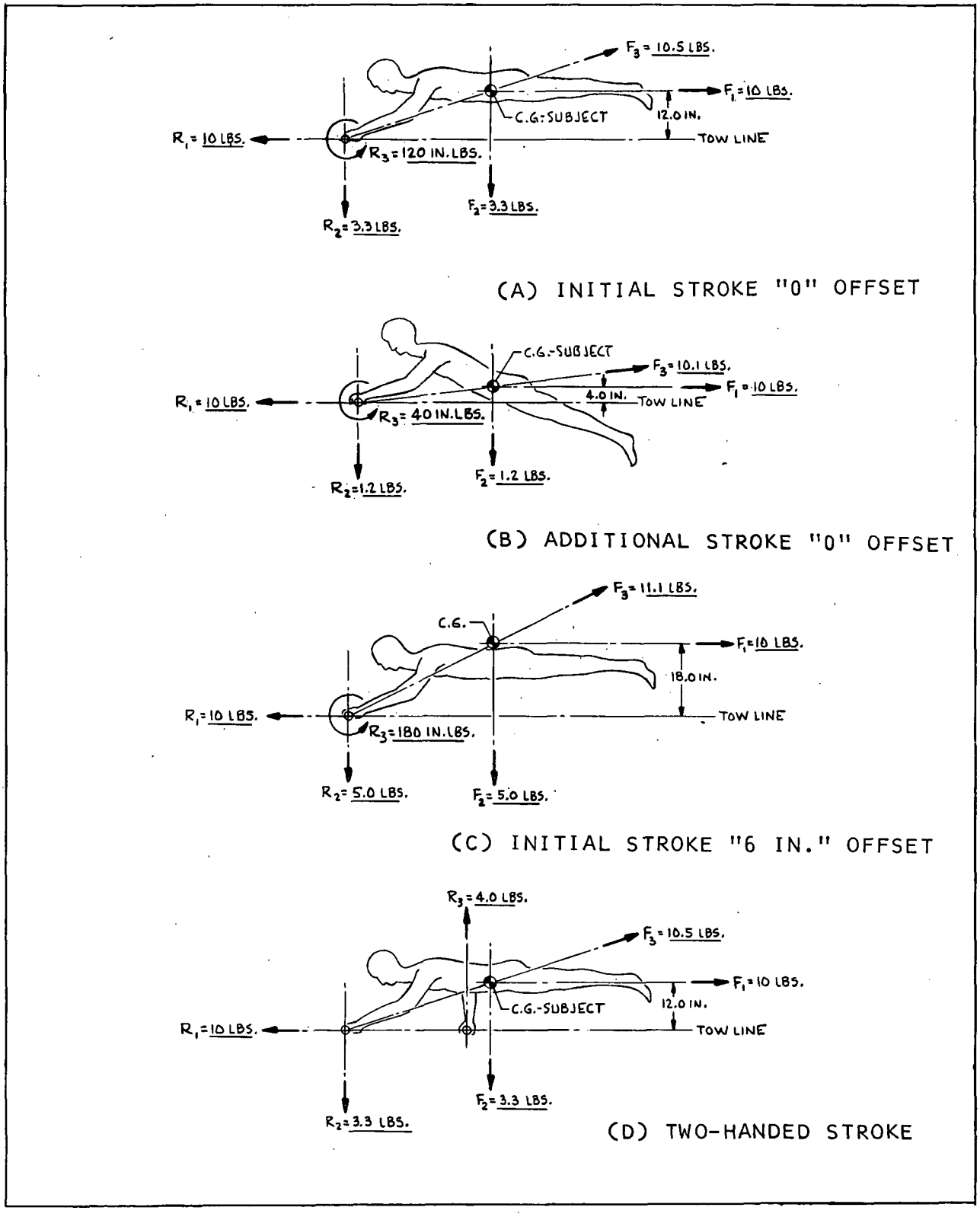

FIGURE 7 - INSTANTANEOUS FORCES ON SUBJECT DURING TRANSPORT MANEUVER

subject closer to the motion aid. In deceleration, however, the requirement for this technique becomes relatively important with increase of mass or shift of mass center away from the motion aid.

The sketches of Figure 7 all depict an instant at which the resultant linear force on the motion aid totals 10 lb. Actually, the situation is dynamic rather than static, and when the subject has reached an instant at which he is applying a 10 lb force, he has already put energy into the system and is actually in some motion. Typical force profiles during acceleration and deceleration are depicted in Figures 8 and 9. These profiles show results for several test masses. Modifications of the force profile, with variations in mass level, tend to be time sensitive rather than magnitude sensitive; i.e., the magnitude of force level seems to remain within a reasonably narrow band over a very wide range of masses. (The minimum mass is, of course, the mass of the subject himself, and the maximum mass is 15 slugs which represents a cargo of approximately 10 slugs.) The area under the force curve, on the other hand, varies with the mass being accelerated. A similar effect, the number of strokes required to reach maximum velocity, can be seen on the velocity profile curves.

Instructions to the test subject required him to accelerate to a "maximum controlled velocity" and then decelerate to zero. No attempt was made to follow a particular course, such as crossing the diameter of Skylab or traversing the length of the shuttle cargo module. The test subject was not advised prior to a test run as to the magnitude of the mass he was transporting. The time of each test run, therefore, was independent of all others, and, in general, required a larger number of strokes and a greater time as mass increased.

Graphical plots of the peak forces per stroke vs time for typical test runs are shown in Figure 10, and discussed in the following to illustrate general operational trends. In these tests, the

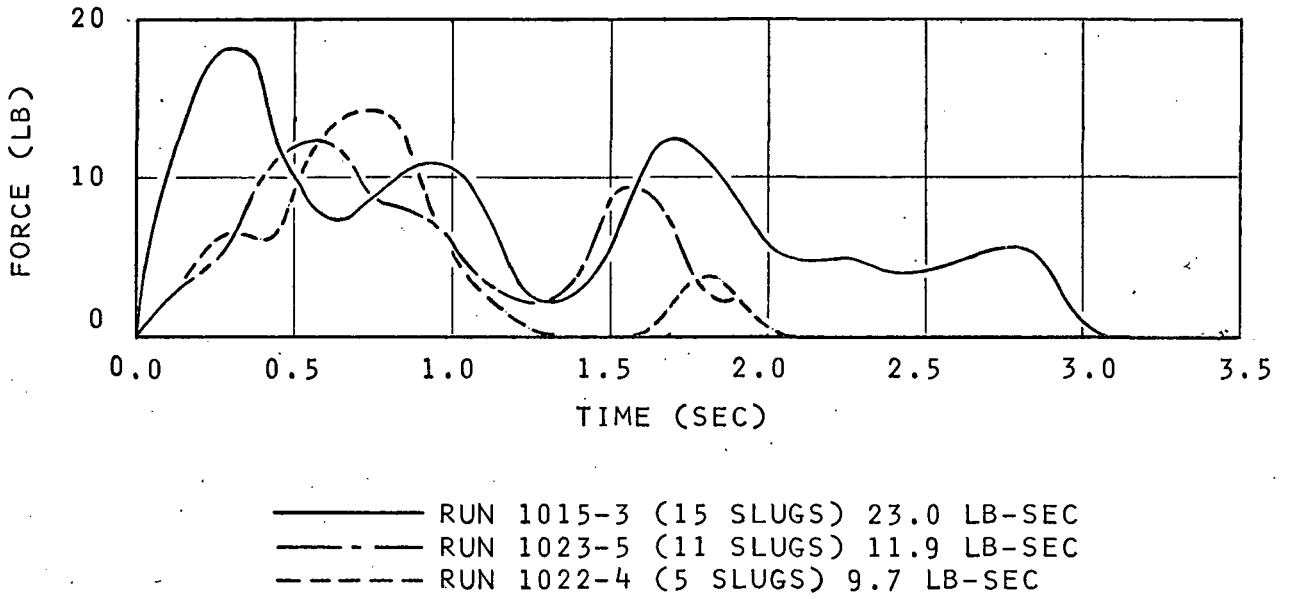

FIGURE 8 - COMPARATIVE FORCE PROFILES--ACCELERATION

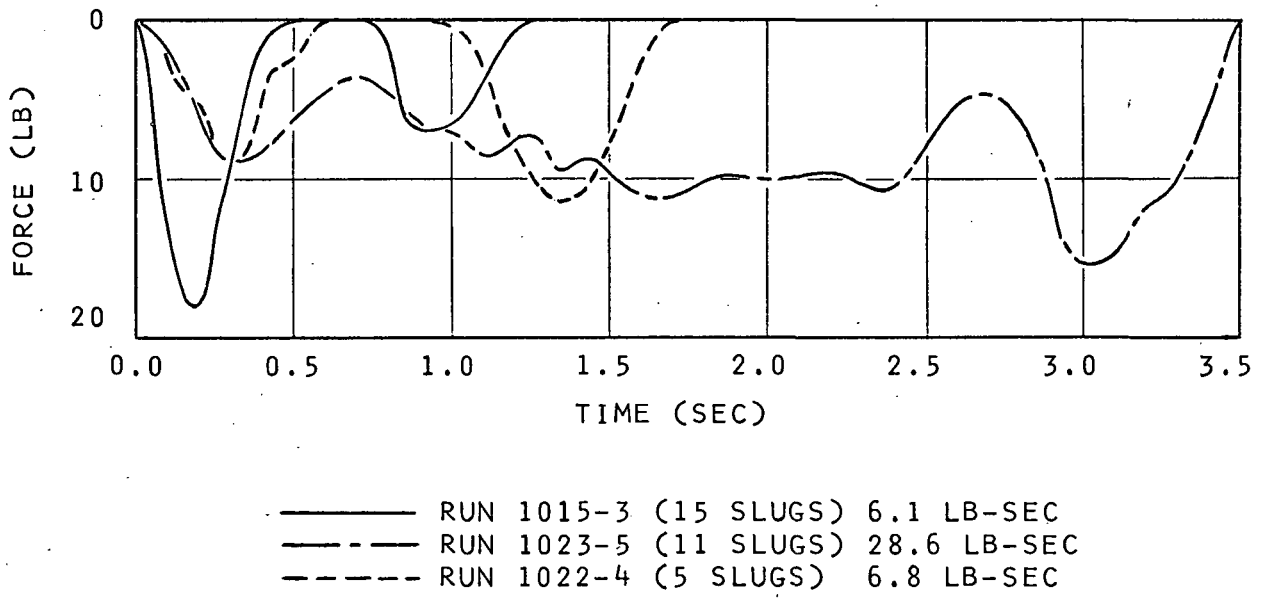

FIGURE 9 - COMPARATIVE FORCE PROFILES--DECELERATION

total mass of the subject and cargo was 15 slugs (cargo mass--10 slugs). The point of attachment in Figure 10-A (Test 1015-3) is at the mass center of the subject (0 offset). The subject was parallel to the motion aid, and used both hands (hand-over-hand) in the general configuration shown in Figure 7-D. The total test time for this particular test was 40.3 sec, of which 26.9 sec were required for the acceleration phase and 13.4 sec for the deceleration phase.

The maximum force exerted during the acceleration period was exerted on the first stroke (right hand). This force was approximately 18 lb. The time of the first stroke was 1.4 sec, at which time the motion aid has accelerated to approximately 0.75 ft/sec. The second stroke (left-handed stroke) required approximately 1.6 sec, exhibited a maximum force of approximately 11 lb, and accelerated the motion aid from 0.75 to 1.25 ft/sec.

Succeeding strokes become shorter and of less magnitude. At the end of 12 sec, a velocity of 3 ft/sec was attained. At that point, additional force application becomes erratic and begins to show deceleration forces intermingled with the acceleration forces. At the end of 24 sec elapsed time, the velocity was 4 ft/sec which was the maximum velocity for this particular test. At 27 sec the subject exerts his first intentional deceleration stroke. The magnitude of this initial deceleration force was approximately 20 lb. Additional deceleration strokes are of less magnitude, and average approximately 5 lb of force. When the velocity was reduced to approximately 2 ft/sec, decelerating forces were increased and reach a maximum of 22 lb of force. In summary, the subject has accelerated with large forces initially, tapering off as velocity increases. After a large initial deceleration stroke, he continues with more moderate forces until velocity is reduced to a point where he can exert larger, more controlled forces.

Figure 10-B (Test 1023-6) shows a test with the point of attachment (simulated system mass center) moved 6 in. outboard. The same general characteristics are evidenced in this test. The initial strokes show higher force levels and longer time periods, whereas succeeding strokes become shorter and of lower force levels. The initial deceleration force again is a higher magnitude than succeeding forces until line velocity is reduced to approximately 2 ft/sec. This test was performed at a later date than the test shown in Figure 10-A, and shows a higher maximum velocity--5.5 ft/sec. The acceleration force profiles are more regular, and the deceleration force is more continuous, resulting in the velocity dropping off more rapidly.

In Figure 10-C (Test 1020-3) the point of attachment is 3 in. outboard of the subject's mass center. In this test, the largest magnitude of force (26 lb) appears on the third stroke. Succeeding strokes were at a reduced level until the final stroke which reached a magnitude of 22 lb, after which deceleration ensued. The deceleration profile is very similar to the previous test (10-B). In each of these tests, three distinct periods appear during deceleration. The first period, approximately one-third of the deceleration time, shows definite stroke characteristics with discernable changes in force level. The second period, again approximately one-third of the total time, shows almost a continuous level of force. The final period exhibits distinct strokes sufficient to cause the line velocity to reach zero.

The three tests, shown in Figure 10, are in chronological order, and are all performed by the same test subject. A comparison of these three tests gives a strong indication of improved subject performance with experience. The early test, 10-A, took 40.3 sec and reached a velocity of approximately 4 ft/sec. The later two tests were performed in a shorter time period, and reached significantly higher velocities. In addition, the pattern of the force profiles during acceleration tends to become more regular

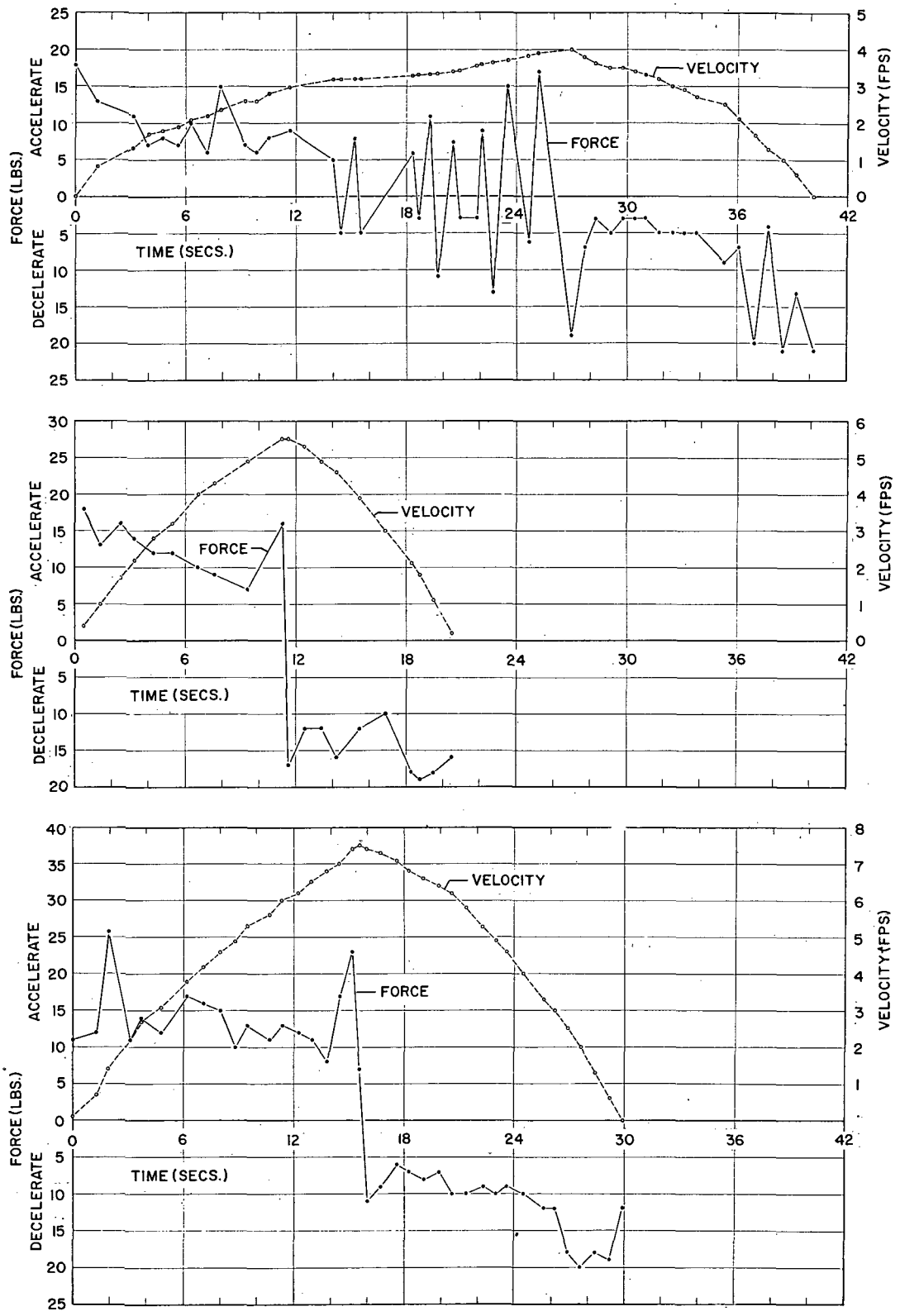

FIGURE 10 - PEAK FORCES VS TIME

with experience, and the subject seems to have established a repeatable deceleration procedure. On the other hand, the force levels for both acceleration and deceleration are approximately the same throughout the test program.

In the previous discussion on Figure 7, Parts A, B, C, and D, it was noted that acceleration forces in general tend to stabilize the subject while decelerating force causes him to become unstable since there is a force component tending to move the mass center away from the motion aid causing the subject to pitch forward. In order to apply a decelerating force, the subject uses both hands in the fashion shown in Figure 7-D, and the time period in between the decelerating strokes occurs as the subject is reorienting his hands for the next stroke. Attempts to decelerate using a single hand caused the subject to pitch forward so that his head contacted the motion aid, and in several familiarization test runs, caused him to pitch a full 180° and/or caused him to lose contact with the motion aid.

3.2 Cargo Transfer Experiment Results

3.2.1 Conventional Water Immersion Simulation Limitations and Theoretical Considerations

Water immersion simulation studies have been used extensively in the past few years to evaluate astronaut performance, to develop EVA tools, support equipment and techniques, and to train astronauts for weightless conditions. This method of simulation has severe limitations, particularly for cargo transfer experiments, that must be considered when conducting zero-G simulations. The major limitations involved are viscous drag, hydrodynamic mass and inertia effects, and accurate neutral buoyancy ballasting of subject and cargo. The effect of these limitations can be minimized, in some instances, with proper simulation design.

Conventional water immersion simulation is primarily limited by three factors:

- .Drag/damping effects.
- .Added mass due to ballast requirements.
- .Preferential attitude imposed by water depth-pressure interactions with fixed ballasting.

The most obvious limitation imposed by the water immersion simulation mode is due to the frictional drag and water viscosity. This drag produces several undesirable effects relative to performance in a true balanced gravity state.

- .Linear and rotational velocities are rapidly attenuated, thus limiting range and dynamics of motion.
- .The drag of the water can be utilized by the subject to provide minor body reactions which would not be possible in a true balanced gravity state.
- .Variation of effective mass of the moving objects as a function of acceleration rate and object form factors.

The potential problems associated with ballasting subject or mock-ups can effect major negative contributions on the simulation results. The ballasting problem is minimal with inert, fixed mass and volume objects. Ballasting of the subject is much more difficult and varies considerably from the case of a scuba-equipped subject, which is very difficult due to the changing volume of the subject as he breathes, to the pressure-suited subject, which is essentially a constant volume case. In the CTS experiments, the buoyancy errors due to breathing of the nonpressure-suited subject are compensated by using a distributed weight device which automatically adds weight in a linear fashion as the subject volume increases due to breathing and subtracts weight during exhale. This is permitted since the subject remains in a quasi-stationary position during a run.

The other two major limitations, viscous drag and hydrodynamic mass and moment of inertia, are dynamic effects on the subject and cargo proportional to their velocity squared and acceleration respectively, and are functions of their shape. Drag forces are the most commonly recognized effects occurring in water immersion studies, and are due primarily to the high viscosity of the water.

In water, velocities greater than 1 ft/sec produce significant drag effects, Figure 11, and must be accounted for in the analysis of data. A means of compensating for drag effects is to determine independently the drag forces on mock-ups and then apply these corrections to data resulting from tests. This is time-consuming and empirical, and thus drag effects are still the most serious limitation in water immersion studies involving translations.

When a body is moved through a fluid (water) which is at rest far from the body, there is kinetic energy associated with the motion of the water as well as with the motion of the object. If the body (the cargo package-mass combination) is moved with varying velocity, there is a corresponding change in the kinetic energy of the surrounding water. The kinetic energy increases as the body does work on the water and decreases when the water does work on the body. This results in the additional drag on the accelerating body, and since the water does work on the decelerating body, a negative drag (thrust) is exerted on the body during deceleration in the direction of motion. The water, in opposing the changes in the body's velocity, acts as if the body has an additional inertia corresponding to an increased body mass. This mass is defined to be the ratio of the kinetic energy of the water surrounding the body to one-half the square of the velocity of the body.

Because of the highly unsymmetric and variable character of the human subject-package combination, precise analytic determination of the effective instantaneous inertia is impractical. These are

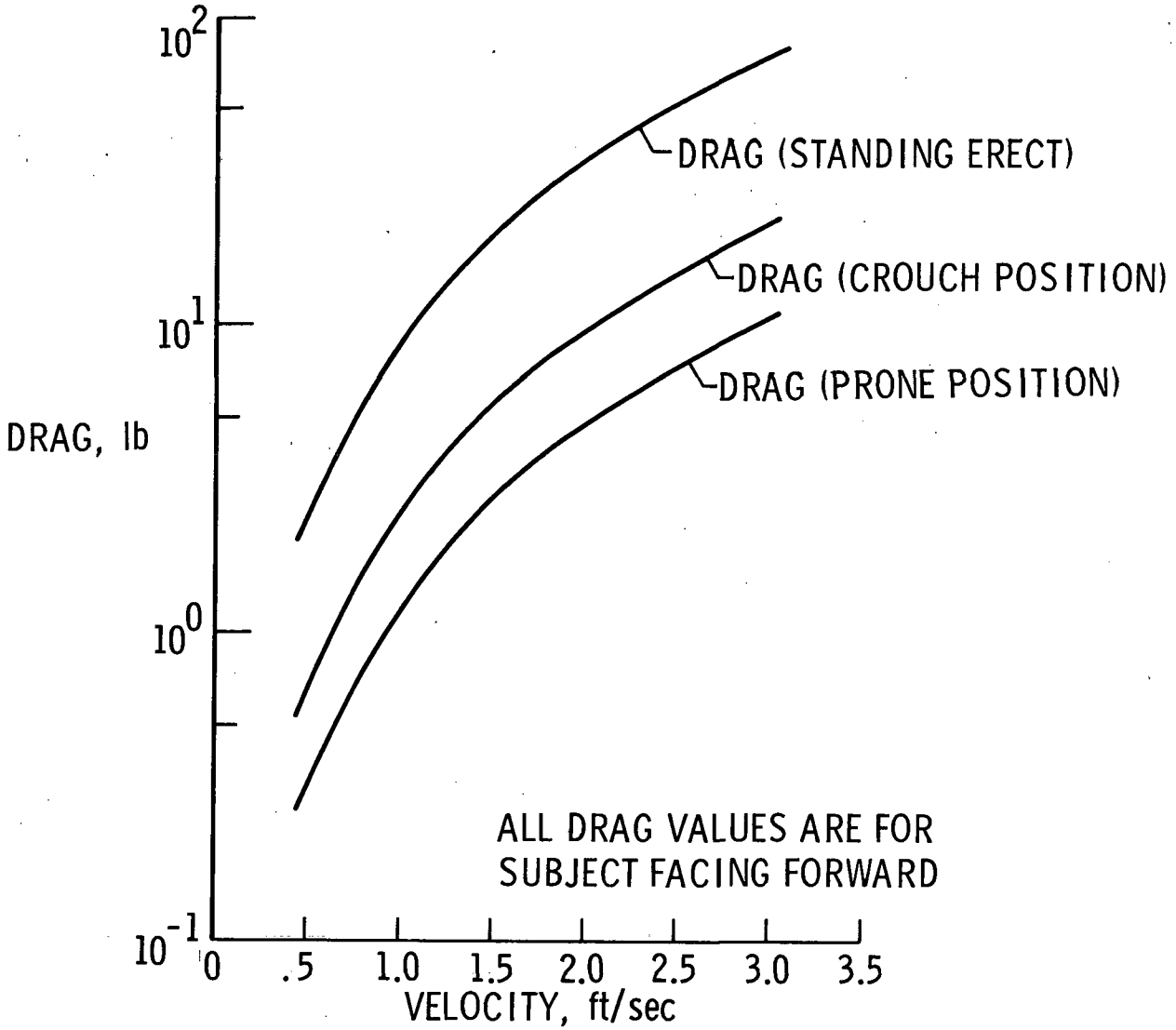

FIGURE 11 - VARIATION OF CALCULATED DRAG WITH VELOCITY FOR WATER IMMERSION TESTS

acceleration-dependent forces, and can increase the apparent mass of the package by 50 percent. In conventional water immersion simulations of cargo transfer, the hydrodynamic mass effects are present during the initial acceleration to a constant transfer velocity and during braking. This area is the least defined of all in water immersion studies, and can be approached only in an empirical fashion, with similar pretest evaluation of the forces involved at different velocities and accelerations for different subject orientations and application of these results to test data. The CTS eliminates these primary effects by transferring the required motion to the motion aid and keeping the subject in a quasi-static state, thereby eliminating motion-induced drag effects. Motion excursions around the mass center are of lower order, and resulting errors are proportionally reduced. Buoyancy errors due to the changing volume during inhale-exhale are compensated for mechanically.

3.2.2 Current Limits for Manual Cargo Transfer

Specific cargo handling simulations have been performed in both the zero-gravity aircraft and neutral buoyancy modes. Initial effort at MSFC,(1)(2) both in-house and contractor-supported, has led to conclusions on package mass-moment of inertia limits on manual (one man) cargo transfer. Quoting from the report,(1) the following conclusions were drawn concerning package mass limitations:

> "Subjects suggested that approximately 41-45 kg appears to be a reasonable maximum for one man to manually transfer, provided the package center of mass is not more than 0.36-0.41 meters from the handhold."

---

(1)Nelson, C. B.: Simulation of Package Transfer Concepts for Saturn I Orbital Workshop. NASA TN D-5111.
(2)Saenger, E. L.: Manual and Automated Extravehicular Cargo Handling Systems--State-of-the-Art. Paper presented at Space Cargo Conference (Long Beach, Cal.), Aug. 3-4, 1970.

Subsequent to this effort, large mass-moment of inertia packages were evaluated at both ERA (on the CTS) and at NASA-LRC in the water immersion facility (conventional water immersion techniques). It has been observed that package mass in excess of 10 slugs does not significantly hamper the ability of man to manually manipulate the cargo. Time constraints and spacecraft IVA geometry would necessarily put a constraint on the operation. The CTS experiments discussed qualitatively in the previous sections were planned to extend this effort and to eliminate uncompensated drag-induced effects, and the specific results are analyzed and described in the following section.

3.2.3 IVA Timelines

A first and practical use of the Cargo Transport Simulator was the development of astronaut IVA manual translation times, both unencumbered and carrying additional cargo. In its present configuration, the CTS can be utilized to provide first-order estimates of the translation times inside the Skylab vehicle complex.

Previous estimates of the unencumbered translation times have been made by the NASA.(3) An updated version of the translation-station-time matrix was received from the COR, and is reproduced in Table II. This table represents essentially the same information as in the document (Ref. 3), except that numerical designations have been substituted for identified letter designations and certain translation stations have been combined. Figure 12 is a pictorial representation of the Skylab vehicle complex with comparative numerical designations for the individual translation matrix cells related to the letter designations from the matrix received from the COR.

---

(3) Skylab Flight Plan--Preliminary Reference. MSC-03625, NASA-MSC, Oct. 1970.

Applying the times in Table II to the approximate distances as shown in Figure 12, it was possible to calculate the average velocity for the transfer between Skylab translation terminals. These velocities are shown in Table III. The relatively wide variation of average velocities, coupled with the restriction of zero mass cargo (unencumbered), gave rise to the requirement for applying the data generated from the CTS experiments to a rationalized estimate of the transfer times for both the unencumbered (0 mass cargo) and cargo handling mode of manual cargo transfer.

In order to directly apply the data to a practical application like the Skylab timeline, an evaluation of prospective cargo configurations and routes was made. This consisted of an analysis of the existing Skylab documentation listed in the bibliography. The analysis was intended to evaluate the most readily identifiable cargo and approximate routes in order to properly constrain the CTS tests.

Table IV is a summary of the results of this analysis, and lists the major cargo elements which have been potentially identified for manual transfer. The table specifically identifies the cargo by weight, transfer terminals, and Skylab descriptor. Where the terminals were not specifically designated, an estimate of the distance to be traversed was made and is designated in the distance column by numbers in parentheses. Where terminals were specified, an approximate average distance was used.

The cargo is classified as to Small, Medium, and Large for subsequent data comparison purposes. These ranges have been arbitrarily established as: Small ($\leq$ 10 lb); Medium ($>$ 10 lb--$<$ 60 lb); and Large ($\geq$ 60 lb). A similar analysis was performed for manual cargo handling for the Shuttle mission by ERA under NASA Contract NAS1-8975-3, and is reported in NASA CR-111847. The results are shown in Figure 13 which divides the potential Shuttle cargo by weight and volume, specifying the frequency (number of packages in each

TABLE II.--ESTIMATED TIMELINE - SKYLAB IVA

		13*	12	11	10	9	8	6	4	3
1 COMMAND MODULE	CM	168	168	168	156	138	108	72	48	36
2 MULT. DOCK. ADAPT.	M	132	132	132	120	102	72	36	12	
4 STRUCT. TRANS. SEC.	ST	120	120	120	108	90	60	24		
6 AIR LOCK MODULE	A	96	96	96	84	66	36			
8 FORWARD DOME	D	60	60	60	48	30				
9 FORWARD COMPART.	F	30	30	30	18					
10 EXP. COMPART.	E	12	12	12						
11 SLEEP COMPART.	S	12	12							
12 WARDROOM	W	12	*WASTE MGT. COMPART.							

NOTES

1. TIMES ARE ESTIMATED IN SECONDS.
2. 0 CARGO MASS.
3. DIRECT TRANSLATIONS.
4. FROM FLIGHT PLAN NOTES: CREW SCHEDULING RECEIVED FROM R. BOND.

TABLE III.--AVERAGE VELOCITIES FOR TRANSLATION BETWEEN STATIONS OF SKYLAB (UNENCUMBERED)

TERMINALS	EST. TIME* (SEC)	APPROX. DIST. (FT)	AVG. VEL. (FPS)	HATCH
1-2	24	12	0.50	X
2-3	12	7	0.58	-
3-4	12	7	0.58	-
4-5	12	4	0.33	X
5-6	12	6	0.50	X
6-7	12	6	0.50	X
7-8	24	7	0.29	X
8-9	30	10	0.33	-
9-10	18	9	0.50	X
10-11	12	10	0.83	X
10-12	12	7	0.58	X
10-13	12	9	0.75	X

*REF. 3
NOTE: X DENOTES ASTRONAUT REQUIREMENT TO TRANSLATE THROUGH HATCH.

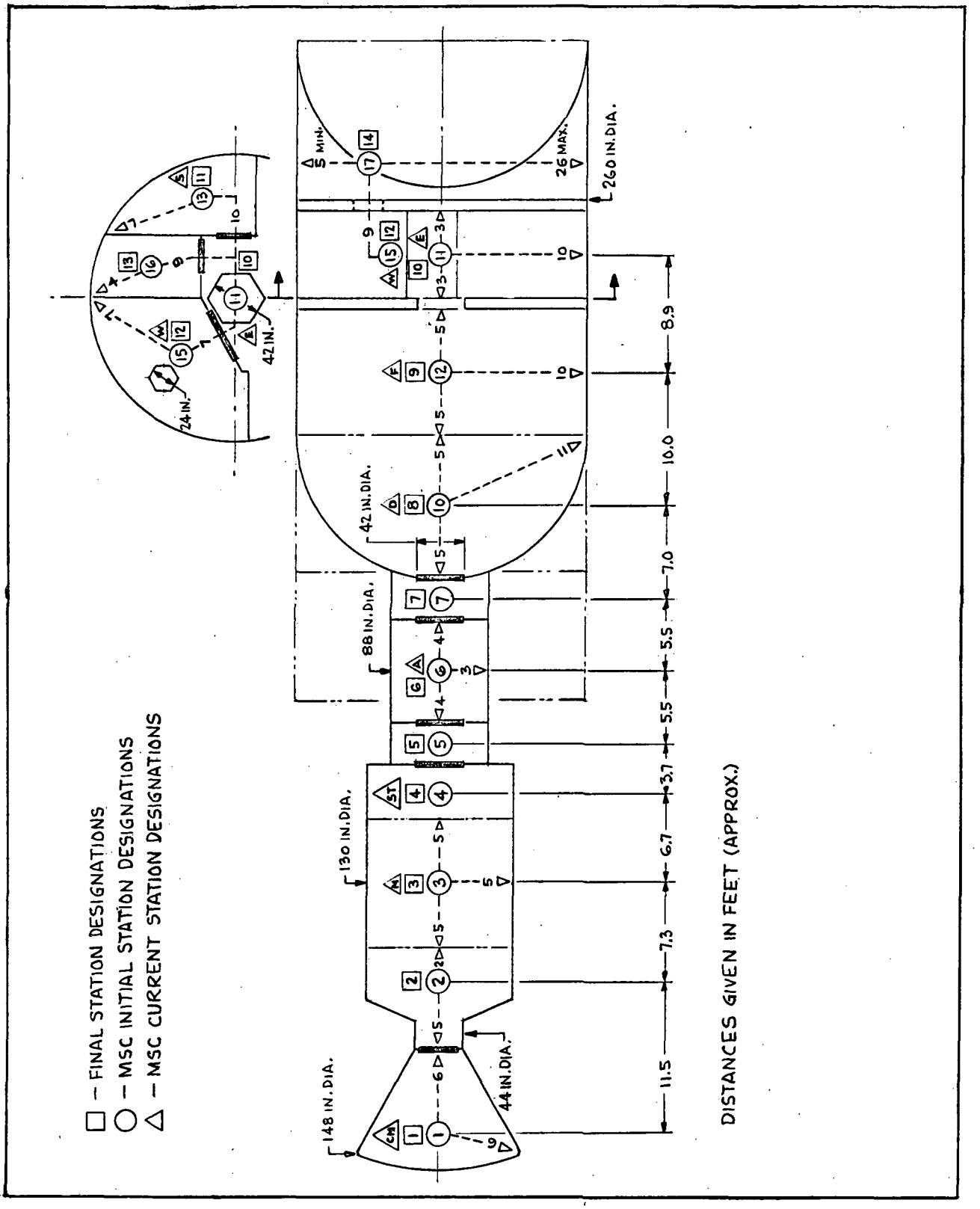

FIGURE 12 - DISTANCES--INTERNAL ROUTES. SKYLAB ORBITAL ASSEMBLY.

TABLE IV.--SUMMARY OF SKYLAB MANUAL CARGO TRANSFER TASKS

DESCRIPTOR	WEIGHT (#)	TRANSFER TERMINAL	CLASS	DISTANCE (FT)
FILM MAGAZINE	4.3		SMALL	
07.001.002-0		12-3		38
07.001.017-0		3-12		38
07.001.019-0		3-12		38
FILM CASSETTE	1.9		SMALL	
07.001.013-0		3-12		38
DETECTOR PACKAGE	30.0		MEDIUM	
08.001.001-0		12-2		46
FILM CASSETTE	2.0		SMALL	
08.002.007-0		12-1		57
PARTICLE COLLECTION MOTOR DRIVE/ CASSETTE UNIT	15.0		MEDIUM	
S149		--		--
OPTICAL CANISTER	22.0		MEDIUM	
08.003.003-0		12		(10)
MIRROR SYSTEM	61.5		LARGE	
08.003.003-0		12		(10)
FILM CANISTER	15.3		MEDIUM	
08.003.003-0		12-1		57
08.003.003-0		12		--
FMSC	18.0		MEDIUM	
08.004.014-0		12		(10)
08.004.015-0		12		(10)
SA	30.5		MEDIUM	
S020		SAL		--
11.009.015-0		12		(10)
UV CAMERA	5.7		SMALL	
08.010.011-0		12		(10)
VERTICAL VISIBLE BRACKET	31		MEDIUM	
08.010.021-0		12-15		15

TABLE IV.--CONTINUED
SUMMARY OF SKYLAB MANUAL CARGO TRANSFER TASKS

DESCRIPTOR	WEIGHT (#)	TRANSFER TERMINAL	CLASS	DISTANCE (FT)
VISIBLE CAMERA ASSEMBLY S063	9.2	WARDROOM WINDOW	SMALL	(7)
MOUNT ASSEMBLY SAL WINDOW FILM MAG. S063	31	--	MEDIUM	--
BATTERIES AND FILTERS 08.010.031-0	1.6	12	SMALL	(10)
ASMU 09.005.001-0	200	12	LARGE	(10)
BATTERIES 09.005.001-0	20.8	12	MEDIUM	(10)
HHMU 09.005.001-0	5.1	12	SMALL	(10)
FILM MAGAZINE M509 11.007.004-0 11.008.001-0 11.008.002-0 11.008.004-0	1.75	-- 12 12 12 12	SMALL	(10) (10) (10) (10) (10)
FILM (60 FRAMES) M509	0.6	--	SMALL	--
PSS 09.005.002-0 09.006.003-0	46.4	 12-7-12 12-7	MEDIUM	 36 18
PSS (CHARGED) 09.005.011-0	50	12-7	MEDIUM	18
FILM 09.006.003-0 10.007.012-0 11.005.002-0	1.5	 12 ?-12 4	SMALL	 (10) -- (5)

TABLE IV.--CONTINUED
SUMMARY OF SKYLAB MANUAL CARGO TRANSFER TASKS

DESCRIPTOR	WEIGHT (#)	TRANSFER TERMINAL	CLASS	DISTANCE (FT)
FILM MAGAZINE, CAMERA, FLOOD LAMPS, CONNECTORS	9.0		SMALL	
T020		--		--
URINE SPECIMEN	0.33		SMALL	
10.001.001-0		1-16		75
DATA TAGS	0.3		SMALL	
10.001.001-0		16-1		75
10.001.001-0		1-16		75
10.001.007-0		16-1		75
10.001.007-0		1-16		75
10.001.012-0		15-1		75
10.001.012-0		1-15		75
VOMITUS BAG	0.08		SMALL	
10.001.007-0		16-1		75
FILM MAGAZINE	1		SMALL	
11.004.003-0 (TESTS 1-12)		4-12-4		64
TESTS 13-37		4-12-4		64
11.004.014-0		4-12-4		64
11.004.015-0		12		(10)
11.004.015-0		12-1		57
11.004.015-0		1		(6)
M151		--		--
11.009.008-0		12		(10)
11.009.013-0		12		(10)
11.009.016-0		12-1		57
S073		--		--
S191		--		--
AEROSOL ANALYZER	7.8		SMALL	
10.010.001-0		11		(10)
10.001.002-0		11-10		19
10.001.002-0		11		(10)
10.001.003-0		11-15		7
10.001.003-0		15-11		7
10.001.004-0		11-16		9
10.001.004-0		16-11		9
10.001.005-0		11-12		9
10.001.005-0		12-11		9
10.001.006-0		11-?		--
10.001.006-0		?-11		--

TABLE IV.--CONTINUED
SUMMARY OF SKYLAB MANUAL CARGO TRANSFER TASKS

DESCRIPTOR	WEIGHT (#)	TRANSFER TERMINAL	CLASS	DISTANCE (FT)
LOG CARDS	0.1		SMALL	
10.001.001-0		11		(10)
10.001.002-0		11-10		19
10.001.002-0		11		(10)
10.001.003-0		11-15		7
10.001.003-0		15-11		7
10.001.004-0		11-16		9
10.001.004-0		16-11		9
10.001.005-0		11-12		9
10.001.005-0		12-11		9
10.001.006-0		11-?		--
10.001.006-0		?-11		--
EXOTHERMIC MOD.	8.2		SMALL	
11.005.004-0		4		(5)
COMPOSITE	0.1		SMALL	
11.005.005-0		4		(5)
SINGLE CRYSTAL MOD.	10.3		MEDIUM	
11.005.011-0		4		(5)
EXPERIMENT SAMPLE STOWAGE CONTAINER	10.1		MEDIUM	
11.005.012-0		4		(5)
11.005.012-0		4-1		26
11.005.012-0		1		(6)
LIMS ASSEMBLY	12.0		MEDIUM	
11.007.002-0		12		(10)
EXOSKELETAL ASSEM.	3.3		SMALL	
T013		--		--
LIMS DATA CABLE	2.5		SMALL	
11.007.002-0		12		(10)
CORONAGRAPH (CANISTER)	19		MEDIUM	
11.008.001-0		12		(10)
11.008.004-0		12		(10)

TABLE IV.--CONTINUED
SUMMARY OF SKYLAB MANUAL CARGO TRANSFER TASKS

DESCRIPTOR	WEIGHT (#)	TRANSFER TERMINAL	CLASS	DISTANCE (FT)
BOOM SECTION	1.5		SMALL	
11.008.001-0		12		(10)
11.008.004-0		12		(10)
HASSLEBLAD 70 MM CAMERA	3.9		SMALL	
11.008.001-0		12		(10)
11.008.004-0		12		(10)
OPTICAL DISPLAY T025	2.5	SAL	SMALL	--
PHOTOMETER SYSTEM	135		LARGE	
11.009.001-0		12		(10)
11.009.008-0		12		(10)
11.009.009-0		12		(10)
11.009.010-0		12		(10)
11.009.013-0		12		(10)
SAL CANISTER	35		MEDIUM	
11.009.014-0		--		--
11.009.015-0		12-1		57
SPECTROGRAPH ASSEM. S183	146	SAL	LARGE	--
FILM CAROUSEL STORAGE CONTAINER S183 (2)	10	CM	SMALL	(6)
CALIBRATION MASSES M179	4.4	WORK AREA	SMALL	--
MAGNETIC TAPE REEL S192 (4)	2.1	--	SMALL	--
RECORDING CAP M133	0.5	13	SMALL	(7)

TABLE IV.--CONTINUED
SUMMARY OF SKYLAB MANUAL CARGO TRANSFER TASKS

DESCRIPTOR	WEIGHT (#)	TRANSFER TERMINAL	CLASS	DISTANCE (FT)
CAP PREAMP & ACCELEROMETER M133 M133	0.5	 13 11F288	SMALL	 (7) --
CENTRAL PANEL ASSEM. M133	15	 --	MEDIUM	 --
TAPE REELS IN CANISTER M133	1.5	 CM	SMALL	 (6)
SAMPLE PANELS D024	0.77	 --	SMALL	 --
CONTAINER D024	5.27	 CM	SMALL	 (6)
CLEAN SOLID TRAPS SOLID TRAP REPLACEMENT	1.0	 --	SMALL	 --
CANISTER MOL SIEVE CANISTER REPLACEMENT	13.2	 --	MEDIUM	 --
CLEAN FILTER FECAL/URINE COLLECTOR ODOR FILTER REPLACEMENT	5.0	 WMC	SMALL	 --
TAPE RECORDER T.R. REPLACEMENT T.R. REPLACEMENT	13.87	 AM 10	MEDIUM	 (5) --
FOOD PACKAGE (12 MAN-DAYS) (3 MAN-DAYS)	 30 7.5		 MEDIUM SMALL	 (20) (20)
UNREFRIGERATED FOOD	200		LARGE	(20)
FROZEN FOOD	50.4		MEDIUM	(20)

VOLUME/ CUBIC FEET

WT/ LB	<1	1-5	6-10	11-50	51-100	101-500	
<1	1						1
1-10	54	4	1				59
11-50	10	49					59
51-100		18	2		1		21
101-500		8	5	6	2		21
501-1000			2	4			6
1001-5000				2	1	1	4
>5000				1	1	1	3
	65	79	10	13	5	2	

COMBINED SPACE STATION CARGO COMPLEMENT

FIGURE 13 - MANUAL PERFORMANCE--PACKAGE DENSITY INTERFACE

class). Superimposed on the matrix are current estimates of man-machine interface, e.g., estimated limits of manual cargo transfer. The unshaded area represents cargo mass-volume generally conceded to fall into the manual range. The lightly shaded region indicates a region of significant current disagreement and includes certain cargo examples from the Shuttle analysis. The dense shaded region represents a reasonable estimate of cargo outside the capabilities of manual transfer. The results of this analysis were used to determine the range of masses to be simulated. For ease of data handling, an upper mass limit of 10 slugs was established, and it was decided to vary the simulated cargo mass between 0 and 10 slugs by 2-slug increments.

In order to eliminate subject error, the test sequence was randomized using a simplified Latin Square technique to prevent information transfer between runs. Table V indicates the technique employed. The six masses were subjected to five random-occurring repetitions for each of the three center of gravity positions chosen.

TABLE V.--CTS TEST DESIGNATIONS AND SEQUENCE FOR TWO-HANDED MANEUVERS

C.G.			TEST NO.					
0	3	6	1	2	3	4	5	6
1012	1017	1022	M6	M4	M2	M1	M3	M5
1013	1018	1023	M1	M5	M3	M2	M4	M6
1014	1019	1024	M2	M6	M4	M3	M5	M1
1015	1020	1025	M4	M2	M6	M5	M1	M3
1016	1021	1026	M3	M1	M5	M4	M6	M2
TOTAL SIMULATED MASS DESIGNATIONS M1 = 5 SLUGS M2 = 7 SLUGS M3 = 9 SLUGS M4 = 11 SLUGS M5 = 13 SLUGS M6 = 15 SLUGS								

The tests were performed as described in the previous section, and the results, Tables VI and VII, were obtained. Due to the subject's interaction with the restraint harness for the vertical (normal) mode tests (Table VII), only the horizontal mode tests were subjected to subsequent statistical analysis. The data of Table VI was subjected to a two-way analysis of variance (ANOVA) to determine the statistical significance of the variation of mass, c.g. offset, and the interaction between the two. The ANOVA was performed for the maximum velocity attained by the subject, the time required to accelerate to the velocity, and the time required to decelerate to zero velocity.

The analysis of variance summaries is given in Table VIII. In general, both the c.g. offset and the mass variation exhibit significant statistical effects both at the 0.01 and 0.05 level. The interaction between mass and c.g. offset was not found to be statistically significant. An interesting anomaly appeared in the significance of c.g. offset for the deceleration time. The lack of significance of c.g. offset is unexplained at present, but possibly could be due to the relatively large magnitude of rotational excursions experienced during deceleration with corresponding increasing random errors to the force inputs to the load cells.

The Row means and the Total means for the average acceleration and deceleration for the two-handed runs are plotted in Figures 14 and 15 as a function of the cargo mass. It must be remembered that the subject's mass must be added to the cargo mass to yield the total mass simulated. An approximate relationship for the acceleration and deceleration as a function of mass was derived and is given below.

$$\overline{A} = 0.75\, e^{-(0.058\, M_c)}$$

$$\overline{D} = 1.26\, e^{-(0.094\, M_c)}$$

where $\bar{A}$ is the average acceleration in ft/sec^2.

$\bar{D}$ is the average deceleration in ft/sec^2.

M_c is the mass of the cargo in slugs.

A simple algorithm was developed to produce a linearized estimate of the Skylab timeline as a function of mass. It consisted of summing individual "free-transfer" time segments for transfer between terminals, assuming an acceleration and deceleration maneuver at every bulkhead which has a hatch-type restriction, i.e., the MDA/AM hatch, the AM/OWS hatch, etc. The average acceleration derived as a result of the CTS experiments was used. Further, it was assumed that acceleration occurred over an arbitrary (approximately one stroke) distance (2 ft), and that the astronaut would free-coast to the proximity of the obstruction (hatch-bulkhead) and apply the subsequent experimentally determined average deceleration.

No estimate was included for passage through the hatch to accommodate comparison with the estimates of Table II. Specifically, the computations comprised computing and summing a $T_{ij}(m)$--time for translation between Terminal i and Bulkhead j; T_{jj+1}--time for translation between Bulkhead j and j+1 for all $j+1 \leq j$ final; and a T_{j_f, i_f}--time for translation between the final bulkhead and the final terminal.

The resulting linearized timeline estimates for 0, 6, and 10-slug cargo masses are given in Table IX. The timelines are linear in the sense that only straight line motions are considered. A graphic comparison of the results for 0 cargo mass is shown on Figure 16 which shows the relationship of the estimated transfer time to Table II to those using the experimentally derived data. Figure 17 shows the effect of mass variation on the estimated timelines for translations originating from the CM and the MDA stations. The combined comparison for translations beginning at the MDA station is shown on Figure 17. Superimposed on Figure 17 are lines of

TABLE VI.--CARGO TRANSPORT SIMULATOR RESULTS

C.G. 0 ALONG ROPE MODE			HORIZONTAL (OVER ROPE) ACCELERATION/DECELERATION TWO HANDS			
MASS (SLUGS)	RUN NO.	V_{MAX} ('/SEC)	T_{ACC} (SEC)	T_{DEC} (SEC)	F_{ACC} (#)	F_{DEC} (#)
5	1012-4	6.0	21.9	6.0	14	12
5	1013-1	6.4	21.5	4.0	14	26
5	1014-6	4.7	16.1	8.9	19	22
5	1015-5	8.4	8.0	5.8	21	18
5	1016-2	8.6	8.8	5.6	15	16
7	1012-3	6.9	6.4	5.1	23	20
7	1013-4	5.0	22.5	6.8	12	26
7	1014-1	5.8	20.8	6.6	13	23
7	1015-2	5.6	20.1	8.1	17	19
7	1016-6	8.0	12.3	8.1	26	14
9	1012-5	5.6	19.8	9.0	18	18
9	1013-3	5.1	21.2	8.8	22	26
9	1014-4	4.2	22.8	8.1	14	23
9	1015-6	7.7	10.9	8.3	19	18
9	1016-1	8.0	11.1	8.7	24	20
11	1012-2	5.5	20.6	10.9	14	27
11	1013-5	4.8	22.8	7.7	20	25
11	1014-3	4.8	19.0	8.3	18	27
11	1015.1	4.3	20.8	9.2	19	15
11	1016-4	7.6	14.3	10.1	18	18
13	1012-6	4.6	18.3	10.7	20	21
13	1013-2	5.4	22.7	8.9	22	33
13	1014-5	4.4	21.3	8.5	16	22
13	1015-4	4.7	21.1	10.9	16	21
13	1016-3	7.0	14.3	9.3	22	19
15	1012-1	5.1	18.3	9.0	21	26
15	1013-6	4.1	26.1	8.8	18	24
15	1014-2	4.4	25.9	10.7	16	25
15	1015-3	4.2	26.9	13.4	18	21
15	1016-5	7.6	16.5	16.1	24	16

TABLE VI.--CARGO TRANSPORT SIMULATOR RESULTS - CONTINUED

C.G 3 ALONG ROPE MODE		HORIZONTAL (OVER ROPE) ACCELERATION/DECELERATION TWO HANDS				
MASS (SLUGS)	RUN NO.	V_{MAX} ('/SEC)	T_{ACC} (SEC)	T_{DEC} (SEC)	F_{ACC} (#)	F_{DEC} (#)
5	1017-4	8.7	7.8	4.7	18	18
5	1018-1	8.8	8.1	5.3	20	18
5	1019-6	8.7	7.3	5.2	24	13
5	1020-5	8.5	7.8	5.7	16	12
5	1021-2	8.4	8.9	4.7	14	18
7	1017-3	7.6	9.7	7.0	20	24
7	1018-4	8.6	8.5	7.5	20	16
7	1019-1	8.5	9.5	7.7	21	18
7	1020-2	8.5	10.8	7.9	24	16
7	1021-6	8.9	12.2	9.0	20	14
9	1017-5	8.1	8.8	7.4	25	24
9	1018-3	8.0	10.3	9.1	20	18
9	1019-4	8.2	9.1	9.2	29	19
9	1020-6	8.2	11.2	10.5	21	20
9	1021-1	8.5	11.5	10.7	19	16
11	1017-2	7.0	10.3	7.8	17	20
11	1018-5	7.6	11.1	9.8	24	17
11	1019-3	8.2	11.0	10.1	24	22
11	1020-1	7.5	12.5	10.6	18	16
11	1021-4	8.1	12.0	11.3	19	17
13	1017-6	7.3	10.0	10.2	24	18
13	1018-2	6.7	10.6	9.2	24	15
13	1019-5	7.5	12.5	12.0	19	17
13	1020-4	7.6	13.6	14.6	19	17
13	1021-3	8.4	14.5	13.6	19	16
15	1017-1	8.5	7.6	4.9	22	18
15	1018-6	7.2	11.8	13.6	21	22
15	1019-2	7.6	--	11.6	21	21
15	1020-3	7.5	15.8	14.4	26	20
15	1021-5	7.8	15.2	14.2	26	24

TABLE VI.--CARGO TRANSPORT SIMULATOR RESULTS - CONTINUED

C.G. 6 ALONG ROPE MODE		HORIZONTAL (OVER ROPE) ACCLERATION/DECELERATION TWO HANDS				
MASS (SLUGS)	RUN NO.	V_{MAX} ('/SEC)	T_{ACC} (SEC)	T_{DEC} (SEC)	F_{ACC} (#)	F_{DEC} (#)
5	1022-4	6.8	8.9	5.4	14	20
5	1023-1	6.6	9.5	7.4	16	17
5	1024-6	7.2	11.4	7.7	13	13
5	1025-5	7.7	9.0	5.9	16	13
5	1026-2	7.8	9.7	10.2	13	7
7	1022-3	6.6	9.5	5.7	17	20
7	1023-4	6.6	8.7	5.6	14	14
7	1024-1	7.0	8.1	7.1	14	14
7	1025-2	7.1	9.4	7.8	13	16
7	1026-6	7.0	8.6	7.0	16	21
9	1022-5	5.5	10.2	6.9	13	18
9	1023-3	5.9	10.4	6.3	15	18
9	1024-4	6.8	11.6	11.1	12	22
9	1025-6	7.2	10.6	9.2	16	16
9	1026-1	7.2	11.8	7.8	15	22
11	1022-2	6.6	14.9	8.9	21	21
11	1023-5	5.7	11.0	8.4	14	20
11	1024-3	6.1	10.7	7.8	16	21
11	1025-1	6.2	11.5	8.6	18	20
11	1026-4	6.7	10.0	10.6	20	18
13	1022-6	5.3	12.2	7.8	16	21
13	1023-2	5.1	11.1	7.3	12	19
13	1024-5	6.0	11.5	12.2	19	22
13	1025-4	6.6	11.9	17.5	15	17
13	1026-3	6.3	10.2	11.5	18	19
15	1022-1	5.4	14.0	27.7	20	21
15	1023-6	5.6	11.5	9.2	16	19
15	1024-2	5.3	10.4	10.2	24	21
15	1025-3	5.4	11.6	9.6	16	22
15	1026-5	5.1	9.0	8.7	19	21

TABLE VII.--CARGO TRANSPORT SIMULATOR

NORMAL TO ROPE MODE					VERTICAL ONE HAND		
MASS (SLUGS)	C.G. (IN.)	RUN NO.	V_{MAX} ('/SEC)	T_{ACC} (SEC)	T_{DEC} (SEC)	F_{ACC} (#)	F_{DEC} (#)
4.03	0	1002-5	6.9	16.08	--	15	--
4.03	0	1003-2	6.7	14.00	--	17	--
4.03	0	1008-1	5.2	24.28	--	12	--
4.03	0	1009-1	7.5	10.22	--	24	--
4.03	0	1010-1	5.0	--	5.84	--	12
4.03	0	1011-1	5.0	--	3.88	--	27
4.03	6	1005-3	7.0	15.06	--	20	--
4.03	12	1006-3	5.8	22.84	--	17	--
4.03	18	1007-1	5.4	15.44	--	15	--
5.04	0	1002-6	6.4	17.72	--	22	--
5.04	0	1009-2	7.6	14.72	--	36	--
5.04	0	1010-2	5.0	--	11.48	--	13
5.04	0	1011-2	5.0	--	5.20	--	20
5.04	18	1007-2	5.9	21.92	--	13	--
6.72	0	1002-7	6.3	19.68	--	14	--
6.72	0	1009-3	7.3	15.84	--	27	--
6.72	0	1010-3	5.0	--	9.98	--	22
6.72	0	1011-3	5.0	--	5.40	--	23
6.72	6	1005-4	6.4	19.24	--	16	--
6.72	12	1006-4	4.6	24.28	--	13	--
6.72	18	1007-3	4.8	24.40	--	15	--
10.08	0	1002-8	6.5	21.00	--	19	--
10.08	0	1009-4	6.9	19.48	--	24	--
10.08	0	1010-4	5.0	--	17.32	--	15
10.08	0	1011-4	5.0	--	7.36	--	25
10.08	18	1007-4	5.0	29.16	--	16	--
20.16	0	1003-3	5.7	32.16	--	25	--
20.16	0	1009-5	6.2	27.52	--	29	--
20.16	0	1010-5	5.0	--	30.56	--	21
20.16	0	1011-5	5.0	--	13.84	--	32
20.16	6	1005-5	3.3	26.84	--	21	--
20.16	12	1006-5	3.7	45.92	--	18	--
20.16	18	1007-5	4.0	41.20	--	14	--
35.76	0	1002-9	5.7	20.16	--	20	--

TABLE VIII

ANOVA DATA SUMMARY - VELOCITY (FPS)

MASS		C.G. OFFSET (IN.) 0	3	6	MASS SUMS	MASS MEANS
0	Σ	34.10	43.10	36.10	113.30	
	M	6.82	8.62	7.22		7.55
2	Σ	31.30	42.10	34.30	107.70	
	M	6.26	8.42	6.86		7.18
4	Σ	30.60	41.00	32.60	104.20	
	M	6.12	8.20	6.52		6.94
6	Σ	27.00	38.40	31.30	96.70	
	M	5.40	7.68	6.26		6.44
8	Σ	26.10	37.50	29.30	92.90	
	M	5.22	7.50	5.86		6.19
10	Σ	25.40	38.60	26.80	90.80	
	M	5.08	7.72	5.36		6.08
C.G. SUMS		174.50	240.70	190.40	605.60	
C.G. MEANS		5.81	8.02	6.34		6.72

	SS	DOF	MEAN SQUARES
BETWEEN MASSES	26.30	5	5.26
BETWEEN OFFSET	79.62	2	39.81
INTERACTIONS	2.05	10	0.21
WITHIN SETS	58.38	72	0.81
TOTAL	166.35	89	

		F RATIO REQUIRED P = 0.05	P = 0.01
F (INTERACTION)	= 0.25	2.64	4.12
F (OFFSET)	= 49.14	3.13	4.92
F (MASS)	= 25.04	3.33	5.64

BOTH THE C.G. OFFSET AND MASS ARE SIGNIFICANT EFFECTS BOTH AT 0.05 AND 0.01 LEVEL.

TABLE VIII.--CONTINUED

ANOVA DATA SUMMARY - ACCELERATION TIME (SEC) - TAC

MASS		C.G. OFFSET (IN.) 0	3	6	MASS SUMS	MASS MEANS
0	Σ	76.30	39.90	48.50	164.70	
	M	15.26	7.98	9.70		10.98
2	Σ	82.10	50.70	44.30	177.10	
	M	16.42	10.14	8.86		11.80
4	Σ	85.80	50.90	54.60	191.30	
	M	17.16	10.18	10.92		12.75
6	Σ	97.50	56.90	58.10	212.50	
	M	19.54	11.38	11.62		14.16
8	Σ	97.70	61.70	56.90	216.30	
	M	19.54	12.24	11.38		14.38
10	Σ	113.70	63.00	56.50	233.20	
	M	22.74	12.60	11.30		15.54
C.G. SUMS		553.10	323.10	318.90	1195.10	
C.G. MEANS		18.43	10.75	10.63		13.27

	SS	DOF	MEAN SQUARES
BETWEEN MASSES	224.42	5	44.88
BETWEEN OFFSET	1197.41	2	598.70
INTERACTIONS	70.62	10	7.06
WITHIN SETS	772.65	72	10.73
TOTAL	2265.10	89	

		F RATIO REQUIRED P = 0.05	P = 0.01
F (INTERACTION)	= 0.65	2.64	4.12
F (OFFSET)	= 55.79	3.13	4.92
F (MASS)	= 6.35	3.33	5.64

BOTH THE C.G. OFFSET AND MASS ARE SIGNIFICANT EFFECTS BOTH AT 0.05 AND 0.01 LEVEL.

TABLE VIII.--CONTINUED

ANOVA DATA SUMMARY - DECELERATION TIME (SEC) - TDC

MASS		C.G. OFFSET (IN.) 0	3	6	MASS SUMS	MASS MEANS
0	Σ	30.30	25.60	36.60	92.50	
	M	6.06	5.12	7.32		6.16
2	Σ	34.70	39.10	33.20	107.00	
	M	6.94	7.82	6.64		7.13
4	Σ	42.79	46.90	41.30	130.99	
	M	8.58	9.38	8.26		8.74
6	Σ	46.70	49.60	44.30	140.60	
	M	9.24	9.92	8.86		9.34
8	Σ	48.30	59.60	56.30	164.20	
	M	9.66	11.92	11.26		10.94
10	Σ	58.00	58.70	65.40	182.10	
	M	11.60	11.74	13.08		12.14
C.G. SUMS		260.79	279.50	277.10	817.39	
C.G. MEANS		8.68	9.31	9.23		9.07

	SS	DOF	MEAN SQUARES
BETWEEN MASSES	379.98	5	75.99
BETWEEN OFFSET	6.91	2	3.45
INTERACTIONS	33.86	10	3.38
WITHIN SETS	537.43	72	7.46
TOTAL	958.18	89	

		F RATIO REQUIRED P = 0.05	P = 0.01
F (INTERACTION)	= 0.45	2.64	4.12
F (OFFSET)	= 0.46	3.13	4.92
F (MASS)	= 22.48	3.33	5.64

THE RESULTS SHOW A STATISTICALLY SIGNIFICANT EFFECT DUE TO MASS BUT INTERESTINGLY ENOUGH SHOW NO SIGNIFICANCE FOR EITHER C.G. OFFSET OR INTERACTION.

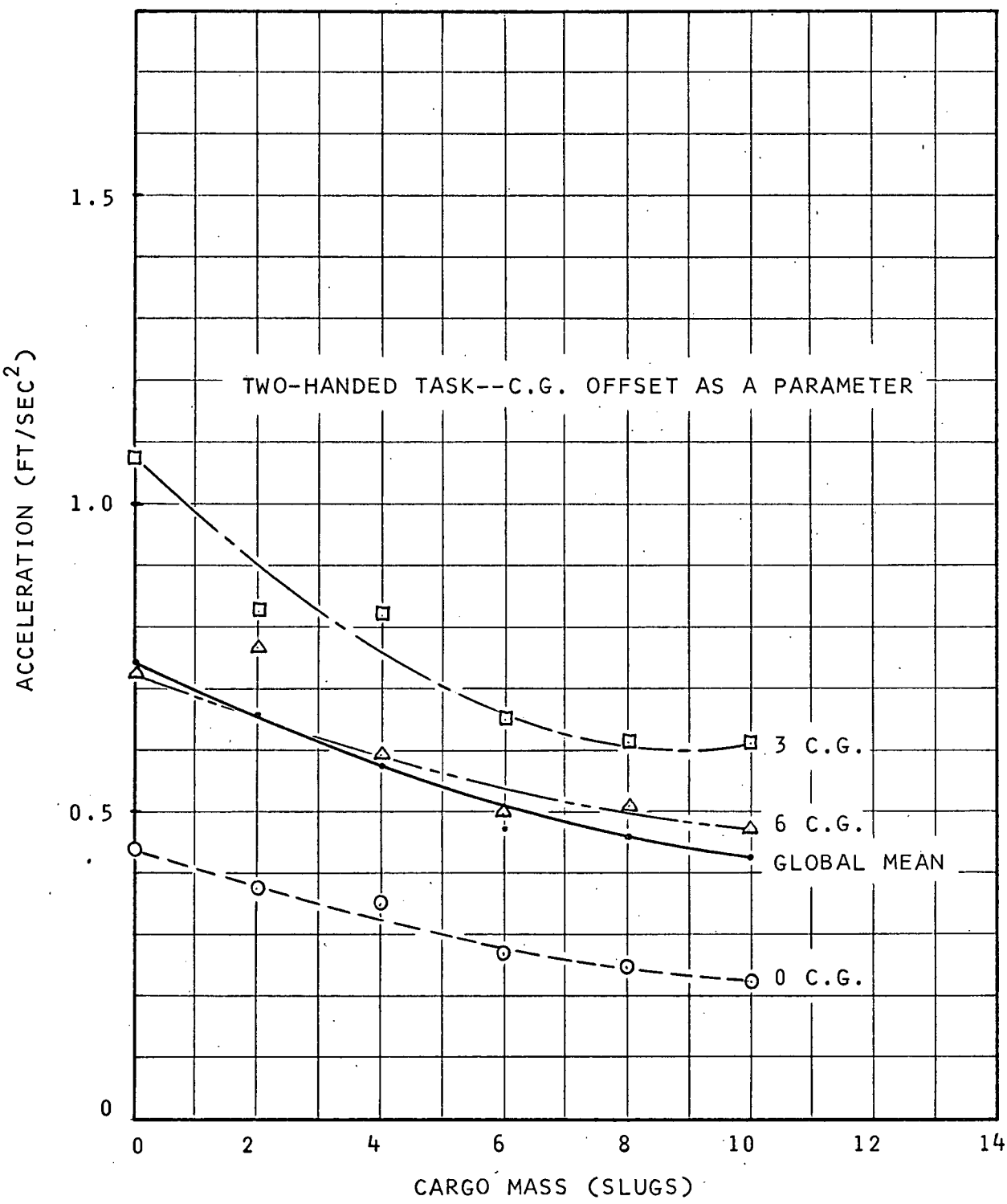

FIGURE 14 - ACCELERATION VS MASS

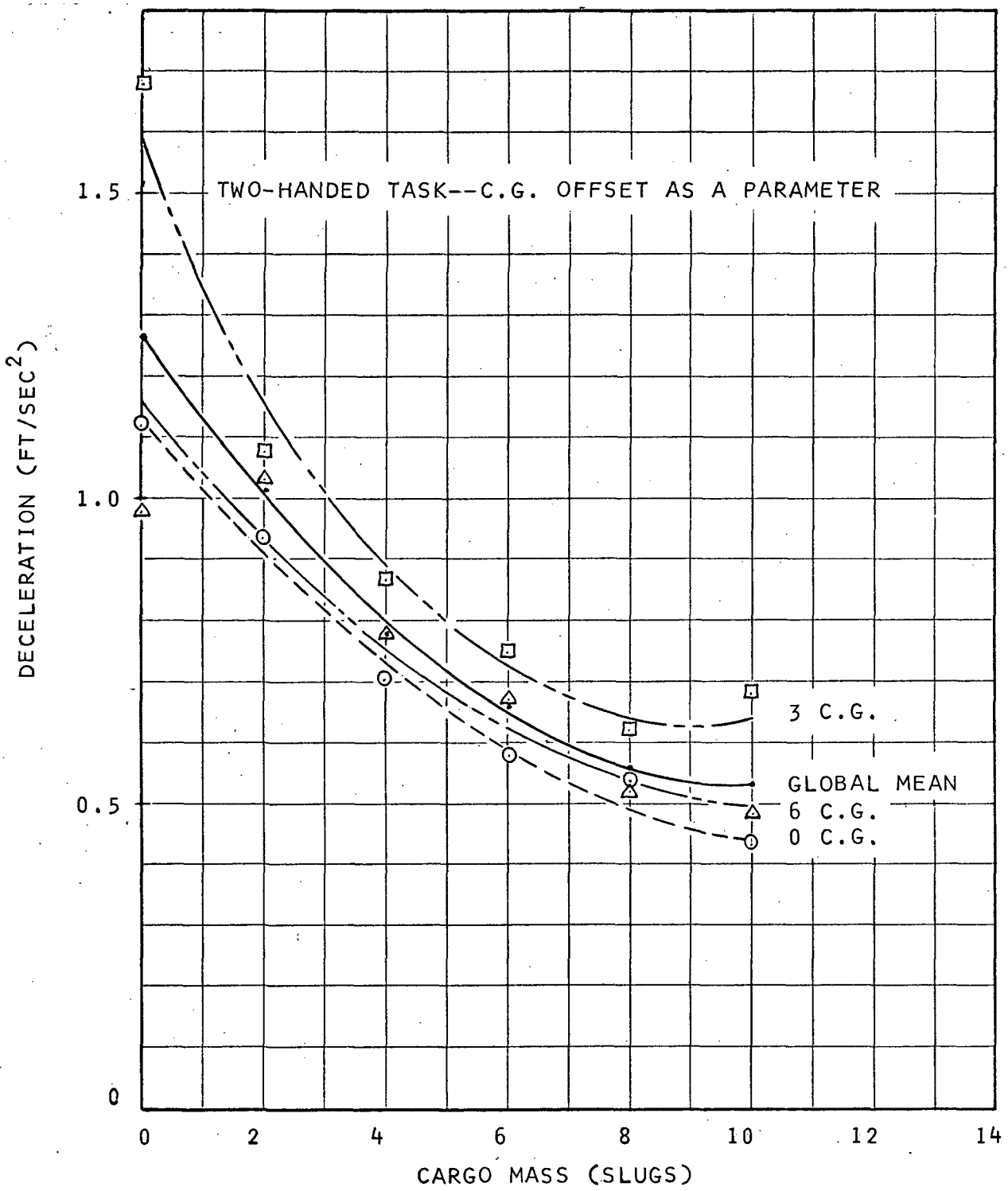

FIGURE 15 - DECELERATION VS MASS

TABLE IX.--EFFECT OF SIMULATED CARGO MASS ON LINEARIZED TIMELINE

	MASS[1]	13[2]	12	11	10	9	8	6	4	3
1 COMMAND MODULE	0	66.2[3]	66.2	66.2	58.9	50.8	43.3	30.6	24.3	17.7
	6	83.2	83.2	83.2	73.7	63.3	53.8	38.2	30.0	22.7
	10	94.8	94.8	94.8	84.2	72.6	63.0	45.9	34.7	25.4
3 MULT. DOCK. ADAPT.	0	50.4	50.4	50.4	43.1	35.0	27.5	15.9	8.5	
	6	63.9	63.9	63.9	54.4	44.0	34.5	20.3	10.7	
	10	72.3	72.3	72.3	61.7	50.1	39.5	23.1	12.2	
4 STRUCT. TRANS. SEC.	0	46.2	46.2	46.2	38.9	30.8	23.3	11.7		
	6	58.8	58.8	58.8	49.3	38.9	29.4	15.2		
	10	66.4	66.4	66.4	55.8	44.2	33.6	17.2		
6 AIR LOCK MODULE	0	36.5	36.5	36.5	29.2	21.1	13.6			
	6	47.0	47.0	47.0	37.5	27.1	17.6			
	10	52.6	52.6	52.6	42.0	30.4	19.8			
8 FORWARD DOME	0	24.9	24.9	24.9	17.6	9.6				
	6	32.3	32.3	32.3	27.8	12.3				
	10	36.0	36.0	36.0	25.4	13.8				
9 FORWARD COMPART.	0	17.4	17.4	17.4	10.1					
	6	22.8	22.8	22.8	13.3					
	10	25.4	25.4	25.4	14.8					
10 EXP. COMPART.	0	7.3	7.3	7.3						
	6	9.5	9.5	9.5						
	10	10.6	10.6	10.6						
11 SLEEP COMPART.	0	14.6	14.6							
	6	19.0	19.0							
	10	21.2	21.2							
12 WARDROOM	0	14.6								
	6	19.0								
	10	21.2								

1 SLUGS
2 WASTE MGT. COMP.
3 SEC

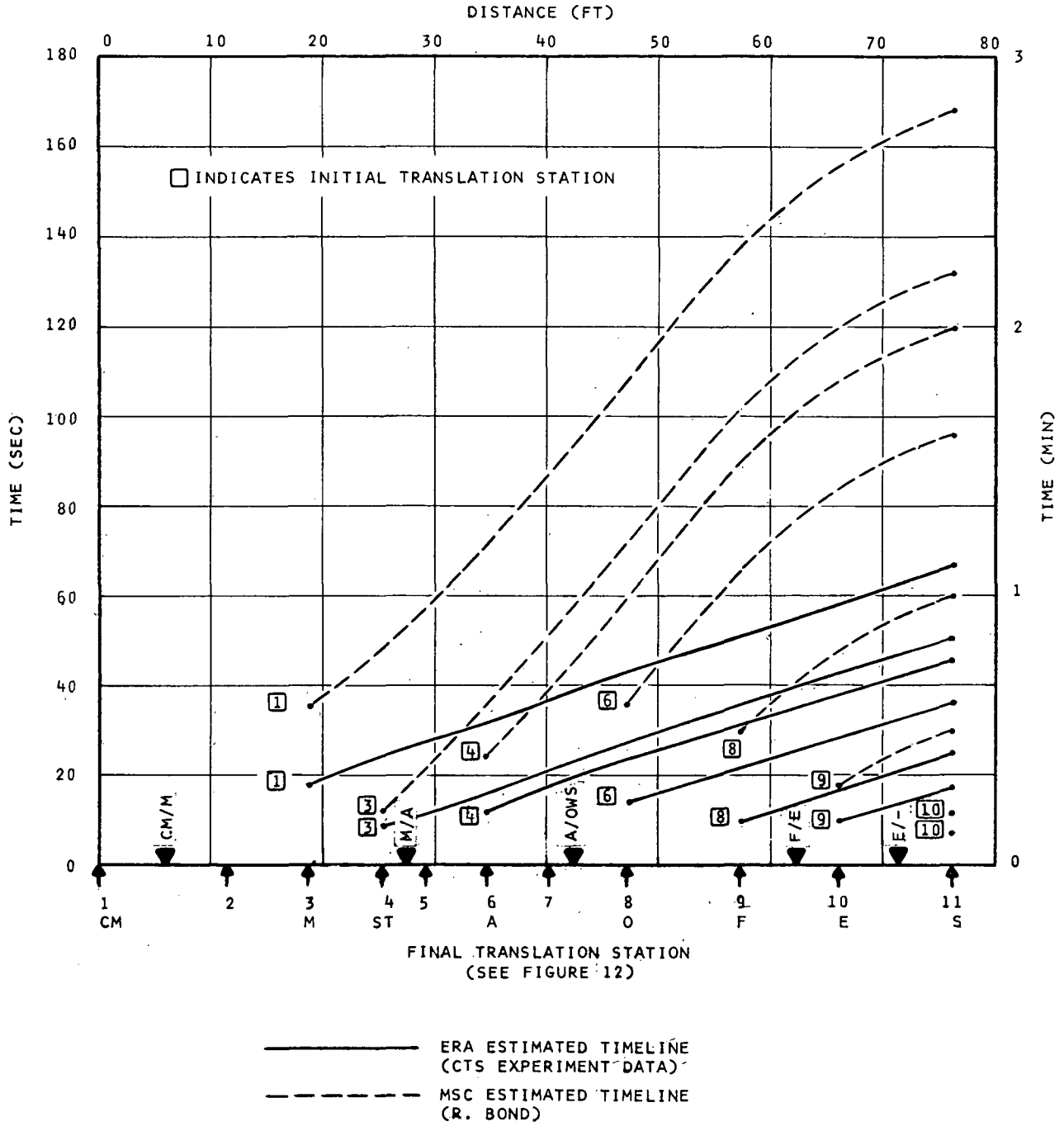

FIGURE 16 - COMPARISON OF TIMELINE FOR 0-SLUG CARGO

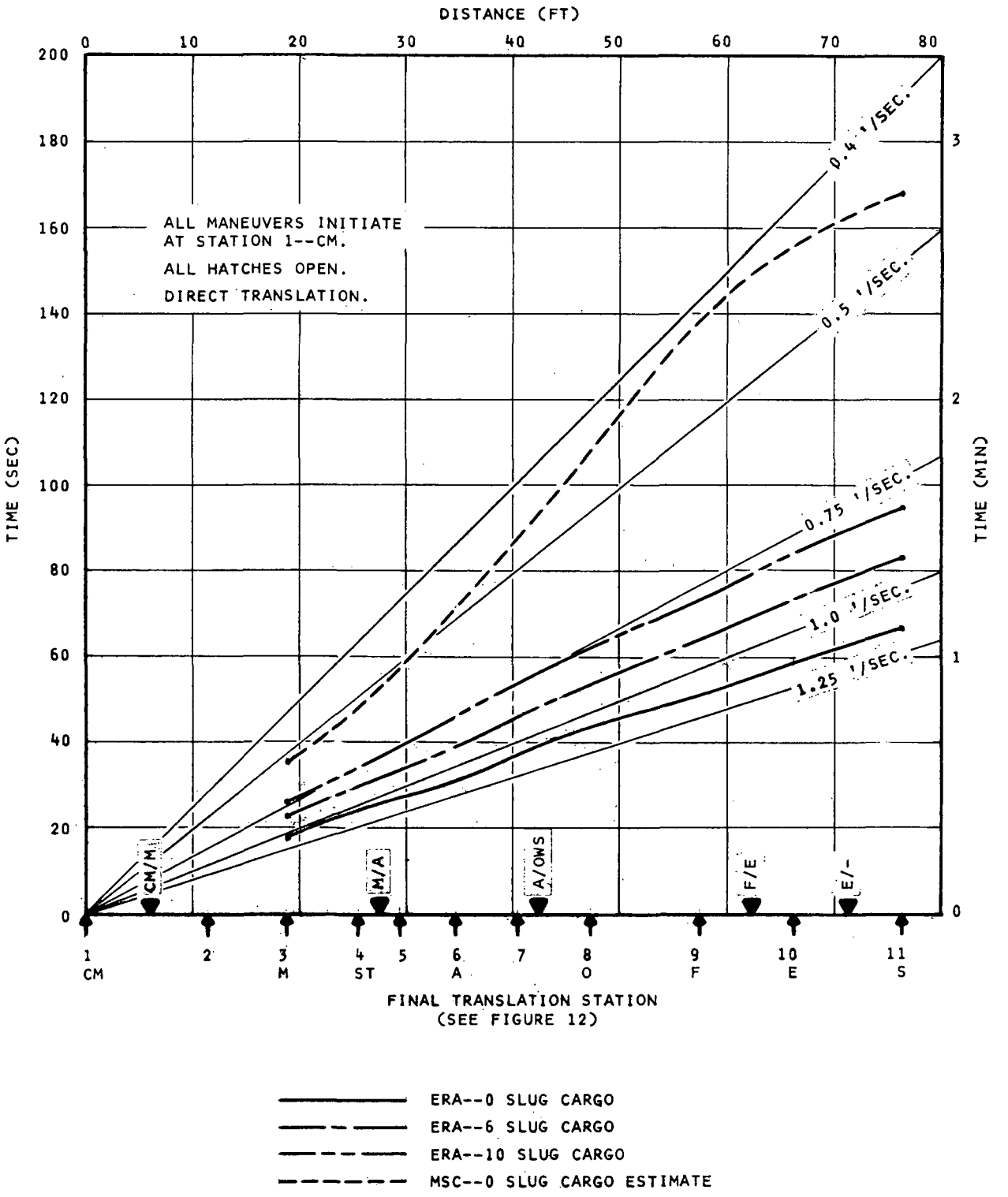

FIGURE 17 - LINEARIZED TIMELINE ESTIMATE

constant average maneuver velocity. It can be seen that the experimental data shows a significant increase in the average transfer velocity for all masses simulated over the estimates of Table II. This factor could be increasingly significant depending on the number and frequency of manned-cargo transfer trips during long duration missions.

3.3 Operational Task Simulation

The development of the Cargo Transport Simulator provides an opportunity to measure human performance under simulated dynamic conditions in weightlessness. The general data from the tests are manual force profiles as a result of a specific motion aid during a translation from one station to another. This has resulted in the development of baseline information for estimating timelines for task performance involving translations and cargo handling. An additional requirement of this contract was to review future missions and select tasks or part-tasks which would be amenable to dynamic simulation utilizing the Cargo Transport Simulator concept. This requirement was partially satisfied by the application of the test data from the CTS to the timelines of the Skylab mission, Section 3.2. In addition, one operational part-task was selected for simulation-demonstration as an application of the simulator concept to tasks other than translation timelines.

The task selected for simulation-demonstration was prompted by a review of the experiments planned for the Skylab missions. There are two Skylab experiments involved. The first experiment, Crew/-Vehicle Disturbances (Skylab Experiment T013), provides a force measuring platform on which an astronaut stands in foot restraints to evaluate disturbances to the spacecraft as a result of body motion. The second experiment, the Foot Controlled Maneuvering Unit (Skylab Experiment T020), provides a thruster unit which the astronaut mounts in such a fashion that he can use his feet to control thruster direction and magnitude. The FCMU will be free

flying inside the Skylab vehicle, and the astronaut will perform a series of attitude control maneuvers and finally a series of translations back and forth across the diameter of the Skylab. This final part-task of translation back and forth across the Skylab in a free flying mode offers an opportunity to measure human performance in weightlessness.

During the performance of the T020 experiment, a second astronaut is required to act as safety man, and positions himself at one terminal of the translation maneuver where he can provide a final arresting of the maneuvering astronaut at his original station and assist him in stowing the maneuvering unit. We recommend that the third astronaut be stationed at the other terminal of the translation maneuver, and also act as safety man in the event that the maneuvering astronaut misjudges his approach to the terminal. At this location, the third astronaut, or safety man, is at the approximate position of the force measuring platform of Experiment T013. If he were to position himself in the foot restraints of the force measuring platform with the recorder on and then provide manual motion arrest or attitude control forces on the maneuvering astronaut, a measurement of the forces required for this maneuver could be made.

Since the astronaut mounted on the Foot Controlled Maneuvering Unit is a greater mass (approximately 11 slugs) than any other mass planned to be handled during the mission, the resultant data, coupled with the planned photographic coverage, would be most valuable in the planning of future tasks.

As an operational demonstration, a simulation was designed to show that a test subject, mounted in foot restraints, could provide the necessary force to arrest an 11-slug mass travelling toward him at velocities up to the maximum possible to attain in the Foot Controlled Maneuvering Unit (2 ft/sec). In the simulation, the test subject was mounted in foot restraints on a platform in a position

normal to the rope motion aid of the Cargo Transport Simulator. The simulator was set to simulate an 11-slug mass, and was put into motion with a velocity of 2 ft/sec. The motion aid was equipped with a target area which the subject could easily identify from a distance of several feet. The subject's task was to arrest the motion aid in one stroke as if he were arresting a free floating mass of 11 slugs approaching at a velocity of 2 ft/sec. In the performance of the task, the subject leans forward as the target area approaches so that he can provide an arresting force over a longer time period. This, of course, minimizes the force level required.

The test results show that the subject decelerated the simulated 11-slug mass without difficulty, and could provide forces up to 30 lb for longer than 1 sec. The results of these tests indicate that the safety men will be quite capable of arresting the maneuvering astronaut from the highest velocity anticipated during the experiment. It should be noted, however, that the test was constructed so that the moving mass reached the safety man at a position approximately 42 in. above the foot restraint platform and approximately 24 in. to the safety man's right. Since the application of arresting force is related directly to the distance from the restraint, a parametric test series would be required to evaluate the safety man's capabilities over a range of situations and potential restraints.

In order to gain additional data from the tests, the platform was equipped with a simple strain gage in an attempt to record the main component of the force profile during the arresting task. This was only partially successful in that the strain gage failed shortly after the tests began. Although the small amount of data recorded prior to equipment failure was not sufficient for useful analysis, it did demonstrate a capability to record data. If there are to be future simulations of this recommended part-task, the instrumentation

for the simulations should include measurement of the force profile at the point of restraint.

3.4 Force Thresholds

In weightlessness, all human manual task performance must be evaluated in terms of specific forces required over specified time intervals to determine the precise requirement for restraints. Tasks requiring only low force applications for short time periods may require no restraint at all, or at least no specialized restraint. Tasks requiring high force applications or low force for long periods generally require restraint. High force applications are limited to the ability of the astronaut to provide peak and sustained forces, and have been the subject of much study and experimental programs by NASA and various contractors. Low force applications, or "thresholds," are not limited in this fashion, and have not yet been properly defined or measured, particularly since they are strongly task dependent. Since it is impractical to include restraints at all the possible locations of low force task performance, it is important to develop a rationale for minimum requirements for restraint or, conversely, the maximum capability without restraint.

The situations demanding investigation are:

1. Long-term personnel emplacement--during tasks which require low force output.

   .Involving low inertia objects.

   .Requiring extreme stability (positional).

2. Working within a confined envelope.

   .Involving high inertia cargo--large forces.

Four distinct experimental variations have been determined which could yield experimental insight as regards thresholds of restraints

in weightlessness. Water immersion experiments could be performed both in a static manner and using the CTS to accomplish the following:

1. Determination of the no restraint-restraint threshold. This is a determination of the force-time profile that an astronaut could provide if he were completely unrestrained (i.e., using only his inertia).
2. Determination of the resistance type force (either as a function of distance or velocity) required for the astronaut to remain within some specified region in space $|\vec{r}| \leq r_o$ over a specified time interval.
3. Determination of the threshold force limit for various restraints by using an arbitrary force error threshold criteria; i.e., the minimum force using a specific restraint for which the astronaut could exert a force described by $F \neq kF$ where k is some arbitrarily selected coefficient ≤ 1. This is predicated on the premise that as the force exerted is made smaller and smaller, the percentage error increases. Determination of the RMS error versus force level for individual restraints.
4. Determination of the minimum rotational velocity threshold for an object exhibiting a variable rotary resistance as a function of restraints.

Using the data from each or all of the above, it would be possible to determine restraint thresholds and breakpoints for the use of different restraints. Although different simulator arrangements would be required for each version, the components and concepts of the CTS would generally provide the necessary data.

4.0 CONCLUSIONS

Five general conclusions can be drawn as a result of the effort performed on this contract.

1. The Cargo Transport Simulator successfully simulated the dynamic conditions of a human translating along a rope motion aid in weightlessness.

   In support of this general conclusions, there are three sources of data.

   A. The characteristics of the force profiles as recorded during the test are analytically predictable. The results of the test series provided numerical values of force applications and frequencies relating to the masses being translated. The linear velocities remained constant during periods of zero force input in contradistinction to the rapid diminution in conventional water immersion simulation.

   B. Subjectively, the simulator provided the responses that one would expect to encounter in weightlessness. Although the simulation is limited visually and degraded by the requirement for breathing apparatus and face mask, the "feel" of the motion aid and resulting body orientations are again what one would anticipate in weightlessness.

   C. Test results agree with orbital experience. In one instance in particular, the tests showed the subjects had a tendency to pitch upward during accelerations which in turn caused their feet to drop below the motion aid. A force analysis showed that this was due to the position of the mass center and the vector of force application. In discussion at Manned Spacecraft Center, it was learned

that this characteristic was encountered by the EVA astronaut of Apollo 9, and that he became concerned that his feet were kicking the side of the spacecraft and that he might cause some damage.

2. Man can provide the motive force to translate both himself and additional cargo in weightlessness.

   The results of the test series performed on this contract show that the force applied by man on motion aids in weightlessness is on the order of 10-20 lb regardless of the amount of mass being translated. The time of translation, however, is greatly dependent upon, and varies directly with, the mass being translated. It was found that man is not a good judge of the forces that he is applying, or of the mass he has accelerated. Therefore, a note of caution must be entered that it appears possible for man to accelerate a large mass to a reasonable velocity (3 or more ft/sec) and then not be able to judge a good stopping or decelerating distance.

3. Realistic rates of translation for man and man with cargo were determined.

   The results of the tests performed on this contract indicate that a realistic rate for man unencumbered with cargo and moving around inside of a sizeable space vehicle, such as Skylab, is on the order of 1 ft/sec. Translating with additional mass attached reduces that rate roughly by a factor of 0.8/unit of mass equivalent to the subject mass.

4. Skylab tasks can benefit from additional studies performed using this Cargo Transport Simulator.

   The particular task used as demonstration of the use of the simulator for future orbital tasks, that of arresting the free flying astronaut FCMU of Experiment T013, was verified.

The techniques used by the safety man to effect a soft capture can be rehearsed and the forces extant measured.

5. The simulator has application as a training device for orbital flight.

A brief review of the onboard film of the Apollo flights indicates that there is a discernable operational learning curve in weightlessness. The astronauts appear to gain confidence with experience in weightlessness, and their movements within the space vehicle appear to be smoother in the films taken later in the flight as compared to the films taken early in the flight. The Skylab crews will be facing a new situation in that the volume of the Skylab will allow them greater freedom of motion, and their early experience may be to provide larger force inputs than are necessary. A training period on the Cargo Transport Simulator may help to reduce the time period for the learning curve in weightlessness, and may serve to identify heretofore undetermined task criticalities.

5.0 RECOMMENDATIONS

The work performed on this contract, coupled with the background of previous studies performed and experience during the Gemini program, leads us to a series of recommendations concerning future efforts which we feel will enlarge the fund of knowledge concerning human performance in weightlessness.

1. The first recommendation concerns continuation of simulations using the Cargo Transport Simulator concept. The test series performed on this contract resulted in data which verifies the simulation technique as a tool for quantitatively investigating weightless operations. This data was used to plot timelines for direct station-to-station manual translation operations, and did not consider courses requiring turns or passage through obstructions or any type of cargo/vehicle interaction. Additional tests should be performed to identify the effect of these characteristics on timelines anticipated for future missions.

2. During this contract, definitions were made of the term "threshold" as it applies to the requirement for restraints and motion aids in weightlessness. A test series can and should be performed to establish values for the various thresholds.

3. The Skylab mission will have human performance experiments which should be comparable to simulations in which force measurements are made to produce hard data. Tasks involving cargo transport on Skylab should be simulated in order to provide a method of postflight comparison and a means of validating simulation.

3. Included in the data reviewed for the performance of this contract was a copy of the onboard films of the Apollo missions. Several sequences from these films have been

useful in determining and verifying velocities of motion and in getting a "feel" for human performance capabilities. There are additional tasks that could be performed inside the Apollo vehicle which would provide additional information for tasks such as human performance experiments on Skylab. Since there are two remaining Apollo lunar flights, we recommend additional planning for the use of the onboard film. Although this would be subject to additional study, there are some obvious possibilities which we can use as examples. First, mass handling in weightlessness. Since this has been the subject of much study, much simulation, and much disagreement, any additional information from flight concerning mass handling would be valuable. The most massive movable object aboard the spacecraft is an astronaut. As a demonstration of mass handling, therefore, one astronaut could curl up in a prenatal position and the second astronaut could demonstrate torquing around the mass center of the object and moving and stabilizing the object. The script for such an operation should utilize a planned camera position and a definite timeline to be followed so that maximum value can come from the film analysis.

A second task which could provide useful information concerning adaptability to weightlessness involves the following: A marble is placed in a three-dimensional maze and maneuvered through the maze from a start to end position. On Earth, this is a manufactured gravity-sensitive device in which the cube containing the three-dimensional maze is maneuvered so that the marble continually falls to the new position. In weightlessness, the maze would effectively be moved around the marble since the marble would not fall. Again, this would require a careful scripting so that maximum benefit could be made of the film analysis.

BIBLIOGRAPHY

1. Ferguson, Ben E. and Anderson, W. M.: Skylab Flight Plan, SL-2, SL-3, and SL-4. MSC-03625, Flight Planning Branch, Flight Crew Support Division, MSC, NASA, 30 Oct. 1970.

2. Papineau, Eugene A.: Skylab Program; Experiment Summaries and Supplementary Data. Martin Marietta, Denver Division, 29 Jan. 1971.

3. Statement of Work for Neutral Buoyancy Testing of Architectural and Environmental Concepts. Spacecraft Design Office, MSC, NASA, 4 Jan. 1971.

4. Orbiting Earth Resources Laboratory Work Station and Restraint Concepts. MSC-01198, MSC, NASA, Apr. 1971.

5. Isom, S. H.: Skylab Operations Handbook. Volume I: Spacecraft Description; Orbital Assembly Module. MDC E0097 (NAS9-11001), McDonnell Douglas Astronautics Co., 20 July 1970, Revised 20 Nov. 1970.

6. Kribs, D. A.: Crew Vehicle Disturbances Experiment Hardware; Skylab Experiment T013; Experiment Operations Manual. MCR-70-49, Rev. A (NAS1-8119), Martin Marietta, 19 Oct. 1970.

7. Beasley, Gary P.: Astronaut Participation in FCMU Water Immersion Simulation Hardware Development. LRC Memo, Langley Research Center, 12 June 1970.

8. Hewes, Donald E. and Glover, Kenneth E.: An Interim Review of Skylab Experiment T020--Foot Controlled Maneuvering Unit. Langley Research Center.

9. Smith, H. T.: Skylab Experiment Operations Handbook. Volume 1: Experiment Descriptions. MSC-00924, MSC, NASA, 9 Apr. 1971.

   Volume 2: Experiment Operational Procedures. 7 June 1971.

10. Karnes, E. W. and Smialek, J. J.: Skylab Program; Experiment Study and Analysis Report; Crew Performance Data Study. NAS8-24000 (MSC-02945), Martin Marietta, Denver Division, 30 Apr. 1970.

11. Karnes, E. W. and Smialek, J. J.: Skylab Program; Experiment M487, Habitability/Crew Quarters, Data/Task Analyses. NAS8-24000 (MSC-03098), Martin Marietta, Denver Division, 29 Oct. 1971.

12. Craw, George W.: Skylab Program; Inflight Operations. Volume I: Status and Index. NAS8-24000 (MSC-00848), Martin Marietta, 31 Mar. 1971.

Volume II, Part 2: Activity Elements.

Volume II, Parts 3 and 4: Activity Elements.

13. Henschke, John M.; Wood, George H.; and Herrick, Dennis E.: Skylab Program; Payload Integration; Skylab Inflight Maintenance (IFM); Task Baseline and Integration Report. ED-2002-1237 (NAS8-24000), Martin Marietta, Denver Division, 15 Jan. 1971.

14. Skylab Stowage List; Operational and Experimental GFE/CFE; Skylab Missions 1, 1/2, 1/3, 1/4. 1-SL-002, MSC, NASA, 16 July 1971.

15. Skylab Stowage List; Command Modules 116, 117, 118; Skylab Missions 1/2, 1/3, 1/4. 1-SL-003, MSC, NASA, 16 July 1971.

16. Skylab Stowage List; Airlock Module; Skylab Mission SL-1. 1-SL-006, MSC, NASA, 16 July 1971.

17. Skylab Stowage List; Multiple Docking Adapter; Skylab Mission SL-1. 1-SL-007, MSC, NASA, 16 July 1971.

18. Skylab Stowage List; Workshop; Skylab Mission SL-1, 1-SL-008, MSC, NASA, 16 July 1971.

19. Experiment Requirements Document for Habitability/Crew Quarters (Experiment M487). ERD-M487, MSFC, NASA, 21 July 1971.